UNITED STATES DEPARTMENT OF THE INTERIOR

GEOLOGICAL SURVEY

Laboratory, Field, and Computer Flow Study of the Origin of Colorado Plateau Type Uranium Deposits

Second Interim Report

by

F. G. Ethridge, N. V. Ortiz, D. K. Sunada, and Noel Tyler

Open File Report 80-805

1980

LABORATORY, FIELD, AND COMPUTER FLOW STUDY OF THE ORIGIN OF COLORADO PLATEAU TYPE URANIUM DEPOSITS

By

F. G. Ethridge, N. V. Ortiz, D. K. Sunada
and Noel Tyler

ABSTRACT

Despite considerable scientific research over the past twenty-five years there still remains much speculation and uncertainty concerning the origin of the so-called tabular uranium deposits of the Colorado Plateau. One particular hypothesis suggests that the deposits resulted from geochemical reactions at the interface between a relatively stagnant solution and a dynamic, ore-carrying solution which permeated the host sandstones. The present study was designed to investigate some aspects of this hypothesis, notably the nature of fluid flow and the relations between the ore deposits and the host sandstones.

Field studies involved an investigation of the character and origin of the host fluvial sandstones and their contained uranium deposits and an examination of the textural and porosity-permeability patterns in similar

Holocene fluvial sand bodies. Data from the Holocene sand bodies was used to construct realistic porous media models. These models were then saturated with a humic acid solution and an aluminum potassium sulfate solution, causing a visible humic acid precipitate to form at the interface of the two fluids. Finally, an existing numerical model was modified and calibrated for use in predicting the shape and location of the interface between the two solutions.

Field observations in the Grants mineral belt led us to concur with the generally accepted hypothesis that the host sandstones (Westwater Canyon Member of the Morrison Formation) originated as a system of braided stream deposits. Detailed field studies by two of the authors in the Slick Rock district of the Uravan mineral belt suggest that the host sediments (Salt Wash Member of the Morrison Formation) originated as channel, point bar, and flood plain deposits of a meandering river system on an alluvial plain. Preliminary results of an examination of the relative proportions of sandstone versus mudstone and channel versus point bar deposits suggests the presence of two major sandstone belts that probably represent the location of major trunk streams that traversed the district in a west to east direction. This conclusion contradicts the generally accepted hypothesis concerning the origin of these sedimentary deposits.

The nature and distribution of the precipitate bands in the porous media flume experiments can be readily explained in terms of texture and porosity-permeability patterns found in Holocene fluvial sand bodies. The similarities between the bands and actual ore deposits in the Colorado Plateau suggest that it is not unreasonable to call upon reactions at the interface between two solutions to produce these so-called trend ore bodies.

Excellent agreement among the numerical, analytical, and physical model solutions indicate the adequacy of the numerical model in predicting the shape and location of the precipitate band in the case of a homogeneous medium.

ACKNOWLEDGEMENTS

The authors wish to express their appreciation to Harry Granger, United States Geological Survey and C. G. Warren, Associate Professor of Chemistry, Colorado State University for their support and encouragement and for their numerous valuable suggestions throughout this phase of the project. The porous-media flume experiments were conducted by James Farentchak. Field and laboratory data on permeabilities, porosities and textural characteristics were obtained by Van Leighton and Richard Johnson. Robert A. Brooks and Robert V. Perry of Energy Reserves Group and John Vanderpool and Bill Pilkenton of Union Carbide kindly provided access to their mines in the Uravan mineral belt. Ellen Winder and Cheryl Knapp provided field assistance to Mr. Tyler in the Uravan Mineral Belt. Fred Peterson provided valuable information on the Morrison Formation in the Colorado Plateau and spent time in the field with the authors. Daniel R. Shawe provided valuable information and expertise on the Slick Rock District. This study was funded by the U. S. Geological Survey, Dept. of the Interior under Grant No. 14-08-0001-G-429. The manuscript was typed by T. L. Ribar.

TABLE OF CONTENTS

LIST OF FIGURES

Figure

LIST OF TABLES

Table

INTRODUCTION AND OBJECTIVES

In the first phase of this study the penetration and precipitation of humic acid into a porous-media flume saturated with aluminum potassium sulfate solution was studied to evaluate one hypothesis concerning the origin of the trend uranium deposits of the Colorado Plateau. In this hypothesis it is suggested that physical and chemical reactions at the interface between two solutions of different composition were instrumental in the formation of the trend* uranium deposits of the Colorado Plateau (Shawe, 1956; Granger, et al., 1961; Granger, 1968, 1976; and Granger and Warren, 1979). In the initial experiments it was first established that a distinct band of precipitate could form at the interface between two solutions. Once this fact was established, the effects of variable flow rates, porous media layering, mudstone lenses (baffles), fluid density differences, and geochemical reactions on the flow phenomenon were evaluated. Results obtained from these investigations are summarized by Ortiz, et al., (1978), Ethridge, et al., (in press) and Ferentchak (1979).

During the second phase of this investigation, data on the sedimentology and the permeability-porosity patterns of Holocene streams were used to design realistic models of these types of deposits for use in the porous media flume experiments. Using these data, additional laboratory experiments were conducted to further evaluate the effects of porous media layering, density differences, and mineral precipitation on the

---

* The term trend deposits as used in this report refers to those types of ore deposits that are distributed along mineralized belts or trends. These bodies are generally tabular in habit and sub-parallel to gross stratification (Bailey and Childers, 1977). They include the so-called peneconcordant deposits (Finch, 1967) and the associated S- and C-shaped rolls (Shawe, 1956).

formation of uranium deposits. The shape and distribution of these simulated deposits and contained precipitate bands were compared with the shape and distribution of ancient fluvial sandstones and their contained uranium deposits in the Colorado Plateau. Finally, an existing numerical model that simulates hydrologic processes was modified and used to predict the shape and location of ore deposits. Results obtained during the second phase of this investigation are described below.

SEDIMENTOLOGY AND PERMEABILITY-POROSITY PATTERNS IN HOLOCENE STREAM DEPOSITS

A. General Statement

Most of the trend type ore bodies of the Colorado Plateau area occur in ancient braided (Grants Mineral Belt) and meandering (Uravan Mineral Belt) river deposits. If, as many authors suggest (Rackley, 1976; Bailey and Childers, 1976; Galloway et al., 1978; and others), mineralization took place shortly after the host sands were deposited, it would follow that these sands would not have been significantly altered by compaction or diagenesis. The distribution of uranium mineralization would then be controlled, at least in part, by the sedimentologic and the permeability and porosity patterns of these ancient river deposits. A better understanding of these patterns in Holocene stream deposits will, therefore, provide valuable data for predicting groundwater flow patterns in ancient fluvial sandstones and the relationships that exist between these deposits and uranium mineralization.

The importance of understanding the sedimentology of these ancient fluvial depositional systems and paleo-groundwater flow patterns has recently been emphasized by Galloway, et al., (1978). Their approach has been primarily to evaluate groundwater flow patterns on a regional basis within a depositional system. Our approach has begun with an evaluation of the characteristics that affect groundwater flow patterns in individual sandstone bodies (river deposits). With this background knowledge (described below) we will attempt to model depositional systems during phase three of this investigation.

B. Field and Laboratory Procedures for Determining Permeability-Porosity Patterns of Holocene Stream Deposits

Permeability-porosity patterns of Holocene sand bodies, including river point bars, beaches and dunes have been investigated by Pryor (1973). The only type of river deposit studied by Pryor was a point bar (meandering river deposit). We have, therefore, used the methodology developed by Pryor (1973) to investigate permeability-porosity patterns in Holocene braided stream deposits of the South Platte River, Colorado.

The two most common large scale deposits of braided stream deposits are longitudinal and transverse bars. Smaller-scale dune bed forms are found in the deeper portions of braided channels. It was, therefore, decided to examine the permeability-porosity and textural patterns of two longitudinal and two transverse bars. However, because of unusually high water conditions, a late winter season in early 1979 and an early winter in late 1979 only two longitudinal bars have been examined to date. Data will be collected on the two transverse bars as soon as the weather and river conditions permit during the third phase of this investigation.

Field and laboratory investigations of the permeability-porosity and texture of braided stream deposits consisted of the following steps:

1) A plane-table topographic map of each bar was constructed.
2) A series of undisturbed and oriented samples were collected in thin-walled aluminum tubes (3.81 cm OD X 7.62 cm long). Samples were collected according to a nested sampling plan similar to that used by Pryor (1973). This type of plan allows assessment of the variation in permeability, porosity, and texture at three different levels of density within the bars. These levels include:
   a) Samples collected at approximately 10-foot (3-meter) intervals in a series of profile lines spaced at approximately 30-foot

(9 meter) intervals transverse to the length of the bar,

b) a grid-pattern of 16 samples on approximately 5-foot (1.5 meter) centers, and,

c) a closely spaced vertical pattern among bedding units in trench faces.

3) Permeabilities of undisturbed samples were measured in the field using a specially built permeameter. Permeabilities were calculated using the following relationship:

$$k = 2.3 \frac{d^2ML}{D^2Pg\Delta t} \log \frac{h_1}{h_2}$$; where:

k = permeability in darcys
d = interior diameter of aluminum tube
M = viscosity (.01386 poises)
L = sample length (7.62 cm)
D = interior diameter of aluminum tube (3.81 cm)
P = density of sample (1.4126 gms/cubic cm)
g = acceleration due to gravity (980 cm/sec^2)
Δt = time in seconds required for fluid level to lower from one height to another in the measuring tube
h_1 = initial height of water in measuring tube above the spillway
h_2 = final height of water in measuring tube above the spillway

4) Samples were then removed from the thin-walled tubes, bagged and saved for laboratory determinations of porosity and grain size.

5) Each sample was carefully weighed in the laboratory and porosity was determined using the following relations:

a) $\text{sample volume } (cm^3) = \frac{\text{sample wt (gm)}}{\text{sample density } (gm/cm^3)}$

b) $\text{pore volume } (cm^3) = \text{sample container volume } (cm^3) - \text{sample volume } (cm^3)$

c) $\% \text{ porosity} = \frac{\text{pore volume } (cm^3)}{\text{sample container volume } (cm^3)} \times 100$

6) Grain size was determined by standard sieving methods (Folk, 1974).

7) A computer program was used to determine mean and medium grain size and sorting from sieve data.

Basic data including sample number, distance from upstream end of bar, porosity, permeability, and grain size statistics for each of the 94 samples collected are given in Appendix I.

C. Point Bar Versus Other Recent Sand Bodies

In his 1973 study, Pryor compared the texture, permeability, and porosity patterns of modern point bar, beach, and eolian sand bodies to each other and to patterns exhibited by artificially packed particles. The results of his study are summarized below:

1) All of these sand bodies have relatively high initial permeabilities and porosities averaging more than 50 darcys and 45% respectively.

2) Permeabilities in the point bars are generally higher and more variable than in the beaches or dunes while porosities are lower and more variable (Table 1).

3) Grain size distribution from the point bar sands are generally coarser and more poorly sorted than those from the beaches or dunes (Table 1).

4) Sand bodies from these three depositional systems exhibit well-organized but somewhat different patterns of variability. Permeability-variation trends are parallel to the length of the point bar sand bodies and perpendicular to beach sand bodies. Dune sand bodies show no particular trend in permeability variation. Permeabilities tend to decrease systematically downstream and bankward in point bar sand bodies.

5) There are wide variations in texture, and hence, in permeability-porosity between bedding units (laminations). However, the vertical

Table 1: Range of values for mean grain size, sorting, permeability and porosity: Longitudinal bars versus point bars, beaches and dunes.

	MEAN GRAIN SIZE (verbal scale)	SORTING	PERMEABILITY	POROSITY
LONGITUDINAL BARS [1]	Fine sand to granule	moderately well sorted to very poorly sorted	1.42 to 202.23 Darcys (av. = 66.14)	27.1 to 53.6 (av. = 41.81)
POINT BARS [2]	Very fine sand to Very coarse sand	well sorted to poorly sorted	40.0 millidarcys to 500.0 darcys (av. = 93)	17.0 to 52.0 (av. = 41)
BEACHES [2]	Fine sand to coarse sand	very well sorted to moderately well sorted	3.6 to 166.0 darcys (av. = 68.0)	39.0 to 56.0 (av. = 49.0)
DUNES [2]	Fine sand to medium sand	very well sorted to well sorted	5.0 to 104.0 darcys (av. = 54.0)	42.0 to 55.0 (av. = 49.0)

[1] See Table 2 for details

[2] Data from Pryor (1973)

and lateral variations within individual laminae are often as great as those between them. This is especially pronounced in point bar sand bodies. Packets of laminae and beds in beach-dune sand bodies are more uniform in character than those in point bar sand bodies.

6) Permeability is directional in cross-bedded units with maximum permeability parallel to the inclined layers (Figure 1).

7) Low permeability clay laminae are common between point bar bedding units and pockets of laminae (Figure 1). These low permeability units will lower the effective permeabilities and hence, the ultimate groundwater through-flow capabilities in these sand bodies.

8) The ideal relations among permeability, porosity, and textural characteristics set forth by Fraser (1935), Graton and Frazer (1935), and Krumbein and Mork (1942) for artificially packed particles are only weakly demonstrated for beach and dune sands and are not demonstrated for point bar sands. Only one of these relations, that of grain size versus permeability is well developed.

D. Braided River Sand Bodies

The two longitudinal bars sampled for this study are located along the South Platte River near Goodrich and Weldona, Colorado (Figure 2). Plan view maps showing topography (Figure 3A and B) reveal that both bars are diamond shaped and have a maximum relief at low water stage of approximately 1 foot (.3 meter). Relief generally increases from the upstream end to the downstream end of each bar.

Both bars have relatively high initial permeabilities and porosities averaging 66 darcys and 42% respectively (Table 1). Permeabilities are less variable than those of point bar and more variable than those of beach and dune sand bodies (Table 1). Average porosities are similar to those found

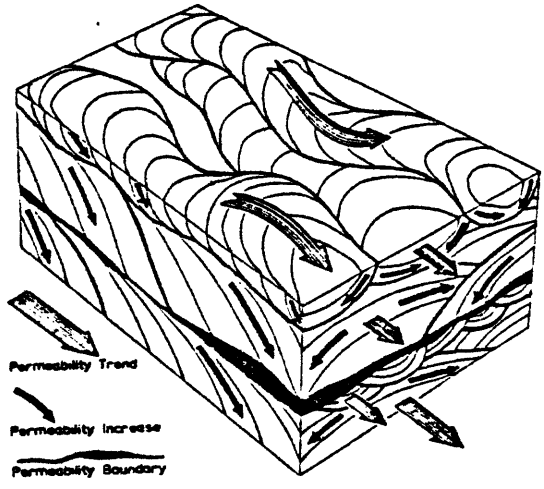

Figure 1. Diagram of river-bar laminae pocket with permeability characteristics (after Pryor, 1973, p. 181).

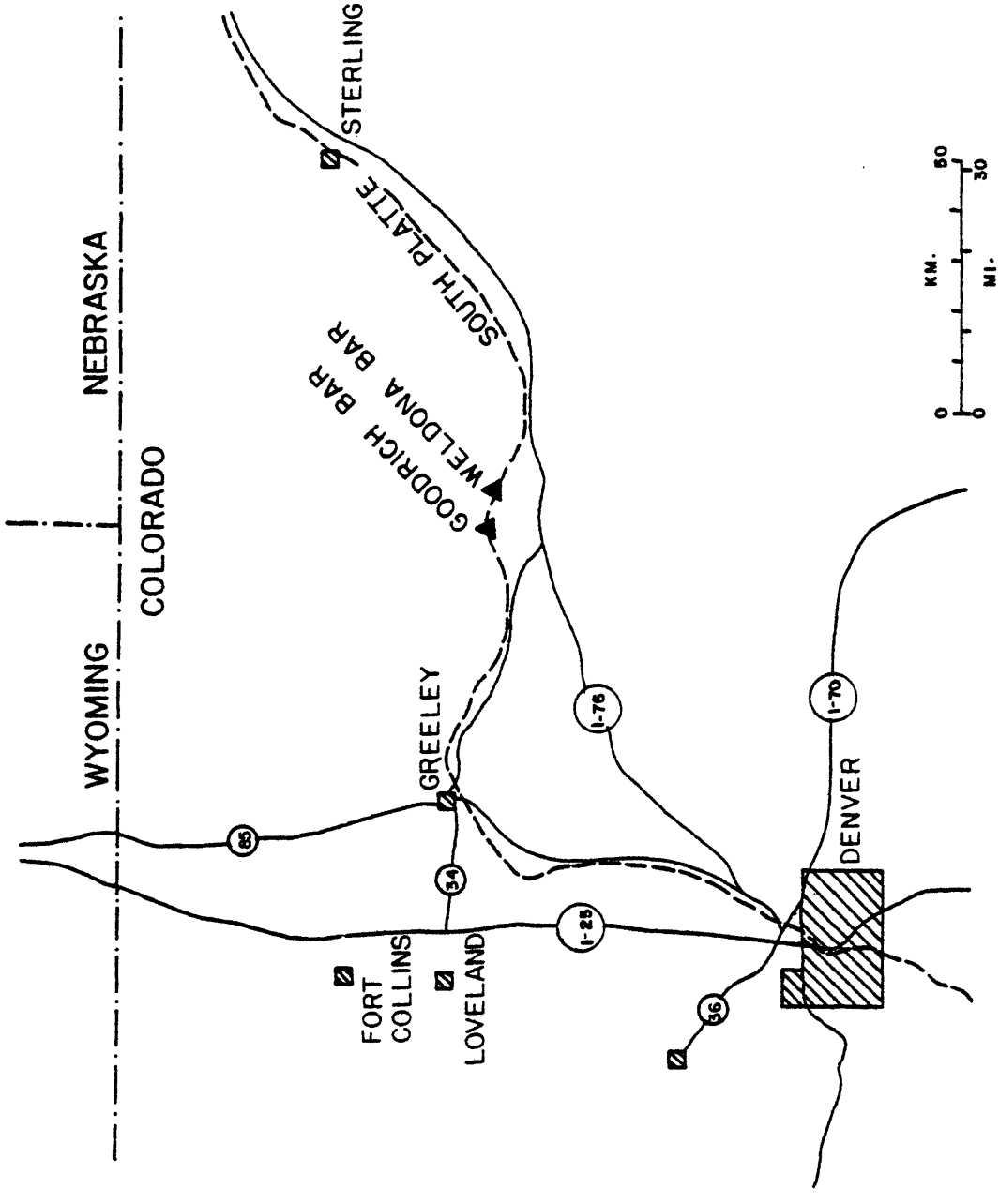

Figure 2. Location map of longitudinal bars 1 and 2. South Platte River, Colorado.

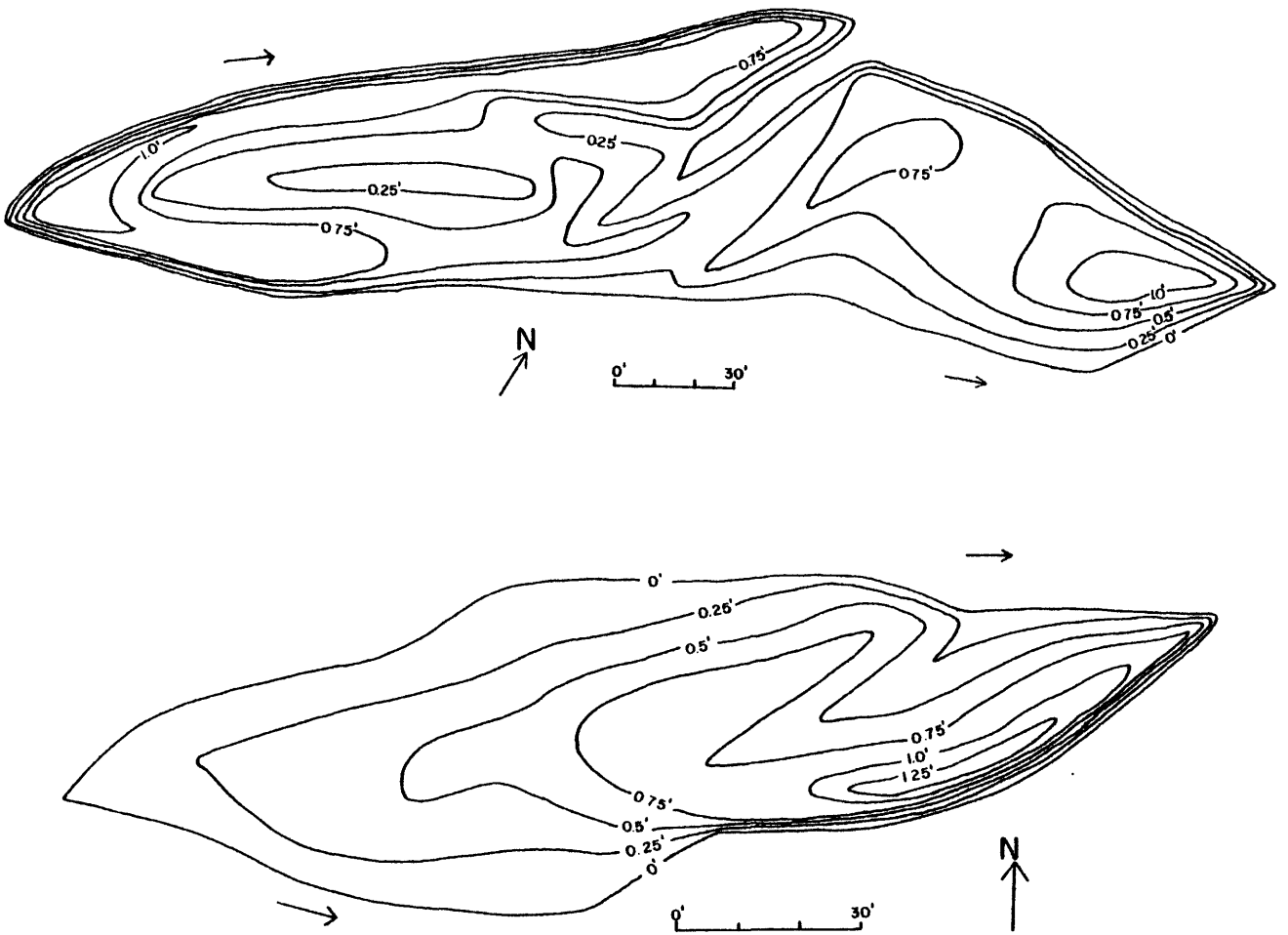

Figure 3. A. Plan view map of longitudinal bar near Goodrich, Colorado along the South Platte River showing topography. B. Plan view map of longitudinal bar near Weldona, Colorado along the South Platte River showing topography. Flow in the South Platte is from left to right.

in point bar sand bodies and porosity variations are less than those found in point bar and greater than those of beach and dune sand bodies (Table 1). Grain size distributions are generally coarser and more poorly sorted than all other sand bodies investigated (Table 1).

In the Goodrich longitidunal bar grain sizes range from 2.8 ϕ (fine sand) to -1.8 ϕ (granule) and average 0.4 ϕ (coarse sand) (Table 2). Permeabilities range from less than 1.4 darcys to 189.5 darcys and average 58.8 darcys (Table 2). Porosities range from 30.9% to 53.6% and average 43.7% (Table 2). Grain size and permeability values tend to be higher and more variable in the highest level of the sampling design (profiles) and lower and less variable in the lowest level (bedding units) while porosity values show the reverse situation (Table 2).

In the Weldona longitudinal bar grain sizes range from 2.1 ϕ (fine sand) to -1.9 ϕ (granule) and averages -0.24 ϕ (very coarse sand) (Table 2). Permeabilities range from 2.8 darcys to 202.2 darcys and average 72.9 darcys (Table 2). Porosities range from 30.9% to 48% and average 40% (Table 2). Grain size tends to be larger in highest level of the sampling plan (profiles) while permeability and porosity values are highest in the intermediate levels (grids) (Table 2). There are no consistent relations between mean values and standard deviation or variance. In fact, the grid samples with the highest porosity have the lowest standard deviation (Table 2). Overall there is no level of the design that shows consistently higher means or standard deviations in terms of grain size, permeability, or porosity, implying that there is as much variation between adjacent laminae or bedding units as there is between the upstream and downstream ends of a bar.

An examination of Figures 4 and 5 will reveal that there is no well organized pattern of variability in permeability or porosity throughout

Table 2. Mean Grain Size and permeability and porosity means, standard deviations and variances for longtitudinal bars, South Platte River, Colorado

Sample Location	NO. OF SAMPLES	MEAN GRAIN SIZE ϕ	MEAN (DARCYS)	ST. DEVIATION	S^2 VARIANCE	MEAN %	ST. DEVIATION	S^2 VARIANCE
Longitudinal Bar #1								
Total	46	+0.40[a]	58.76[b]	40.51[b]	1640.79[b]	43.73	4.00	16.02
Profile	24	-0.056[c]	70.13[d]	43.87[d]	1924.54[d]	41.65	3.66	13.38
Grid	16	+0.64[e]	54.52[f]	31.82[f]	1012.21[f]	45.54	1.74	3.04
Bedding Units	6	+1.65	20.05[f]	13.98[f]	195.24[f]	47.25	4.77	22.76
Longitudinal Bar #2								
Total	48	-0.24	72.90	48.32	2334.34	39.97	4.09	16.73
Profile	18	-0.41	53.98	34.94	1220.67	38.66	3.96	15.71
Grid	16	-0.20	111.45	45.81	2098.20	42.57	2.51	6.32
Bedding Units	13	-0.04	56.11	38.45	1418.76	37.30	9.19	84.45
Both Longitudinal Bars	94	+.062[g]	66.14[h]	45.55[h]	2075.06[h]	41.81	4.49	20.13

[a] based on 43 samples : 3 samples to open-ended to calculate

[b] based on 44 samples : 2 samples w/permeability to low to measure

[c] based on 22 samples : 2 samples to open-ended to calculate

[d] based on 23 samples : 1 sample w/permeability to low to measure

[e] based on 15 samples : 1 sample to open-ended to calculate

[f] based on 5 samples only: 1 sample w/permeability to low to measure

[g] based on 89 samples: 4 samples to open-ended to calculate

[h] based on 92 samples: 2 samples w/permeability to low to calculate

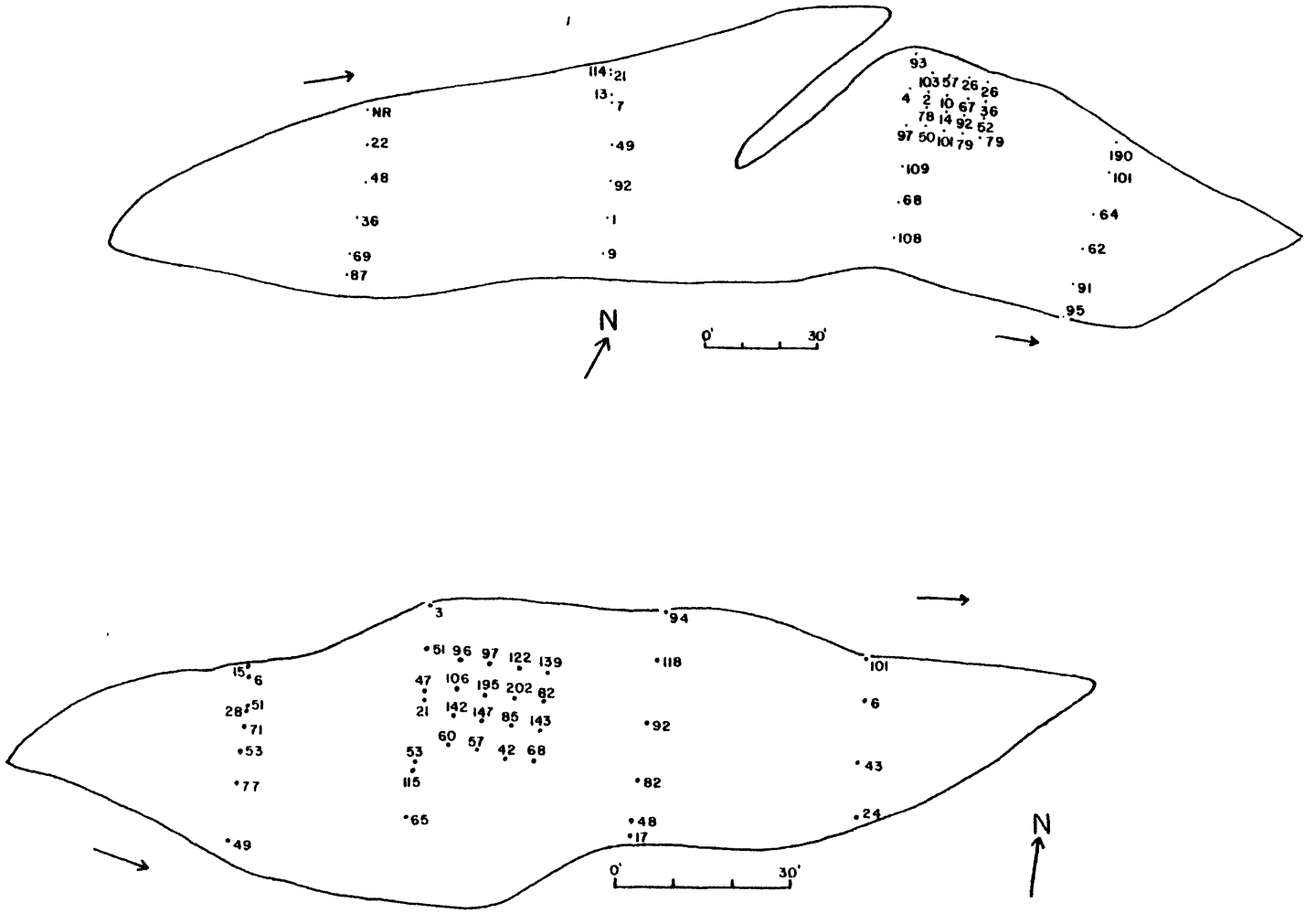

Figure 4. (A) Plan view map of longitudinal bar near Goodrich, Colorado on the South Platte River showing permeability distributions. (B) Plan view map of longitudinal bar near Weldona, Colorado on the South Platte River showing permeability distributions. Flow of river is left to right.

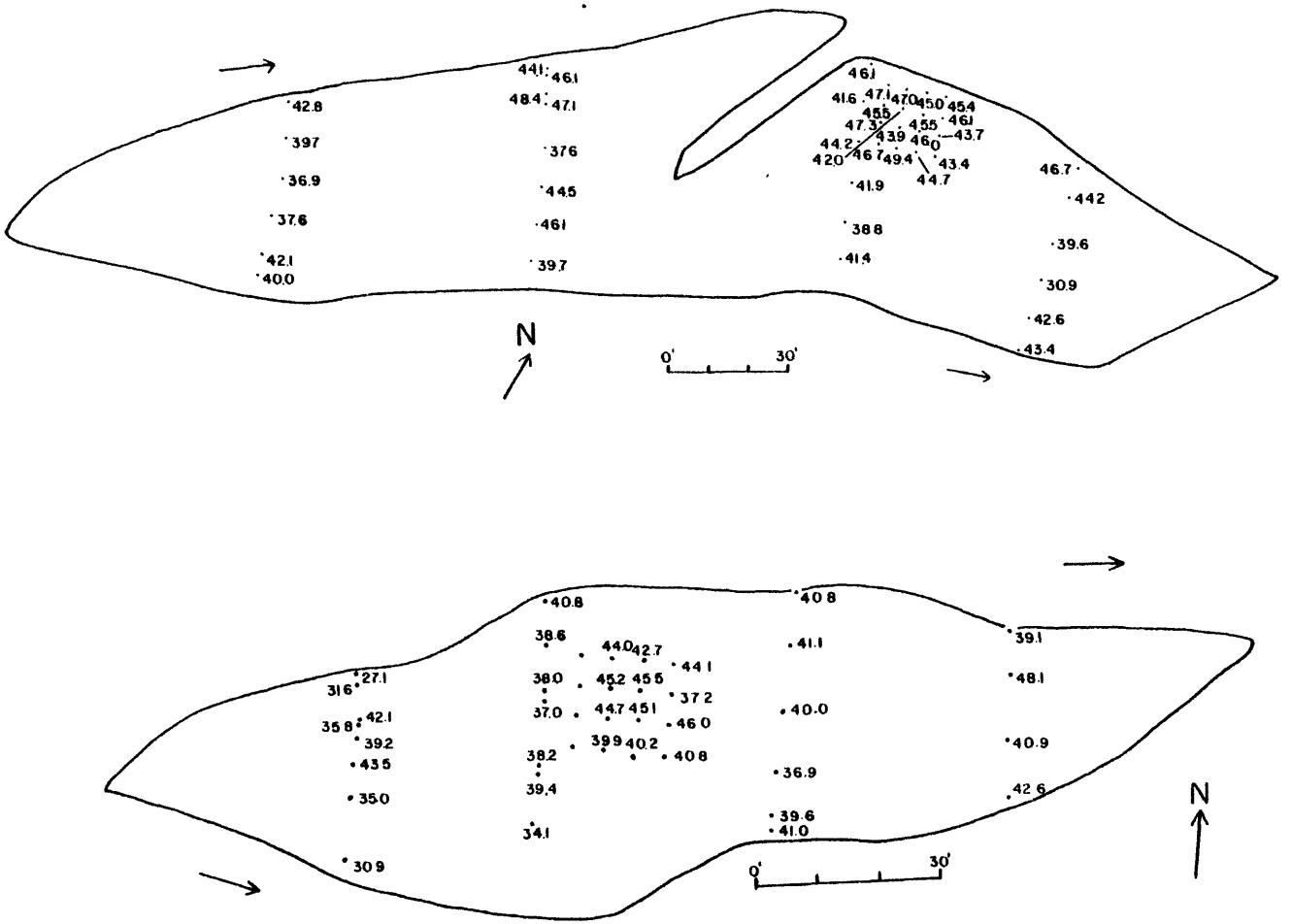

Figure 5. (A) plan view map of longitudinal bar near Goodrich, Colorado on the South Platte River showing porosity distributions. (B) plan view map of longitudinal bar near Weldona, Colorado on the South Platte River showing porosity distributions. Flow in river is from left to right.

the bars. This result is in direct contrast with the significant trends found for point bar and beach sand bodies (Pryor, 1973) and results from the lack of significant overall trends in grain size or sorting within the longitudinal bars.

Because of the general horizontal nature of bedding units within the longitudinal bars and the general lack of cross-stratification, directional permeability is dominantly horizontal. Although clay laminae are present within the longitudinal bars they are not as common or continuous as in the point bar sand bodies. It would follow, therefore, that these low permeability units would not constitute a significant factor in the reduction of effective permeabilities in the longitudinal bar sand bodies. Hence, the ultimate groundwater through-flow capabilities would be greater in these sand bodies than in point bars.

An examination of the relations between permeability-porosity and texture for the longitudinal bar sand bodies reveals the following:

1) A significant exponential increase in permeability with an increase in grain size (Figure 6),
2) a significant decrease in porosity with an increase in grain size (Figure 7),
3) no relation between permeability and sorting (Figure 8), and
4) a significant increase in porosity with an increase in sorting (Figure 9).

It would appear, at first glance, that the ideal relation among permeability, porosity, and textural characteristics for artificially packed particles are not consistent with field data from either the point bar or the longitudinal bar sand bodies (Table 3). Pryor (1973) suggested that the different styles

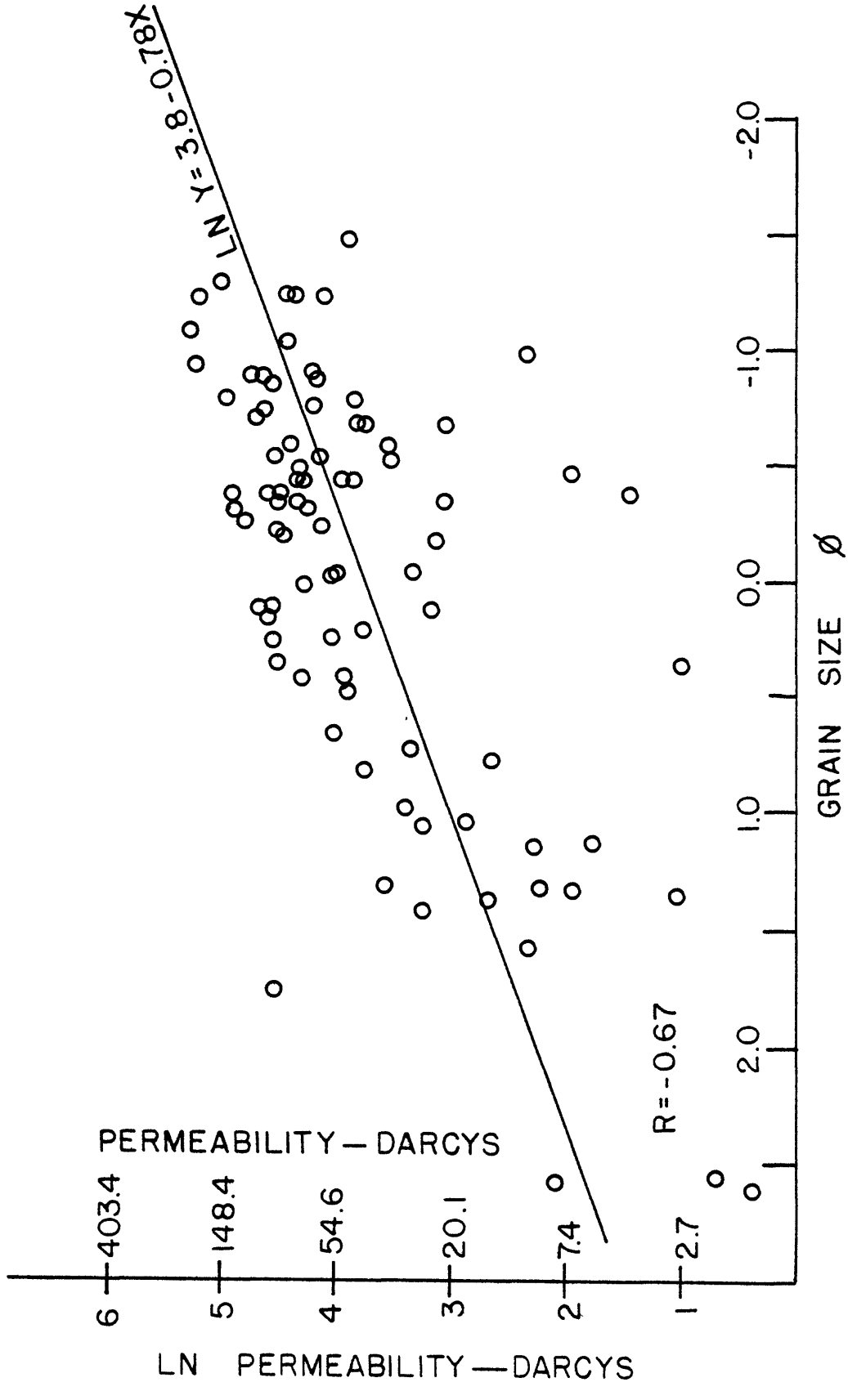

Figure 6. Mean grain size versus permeability. Data from both longitudinal bars on South Platte River. For location of bars see Figure 2.

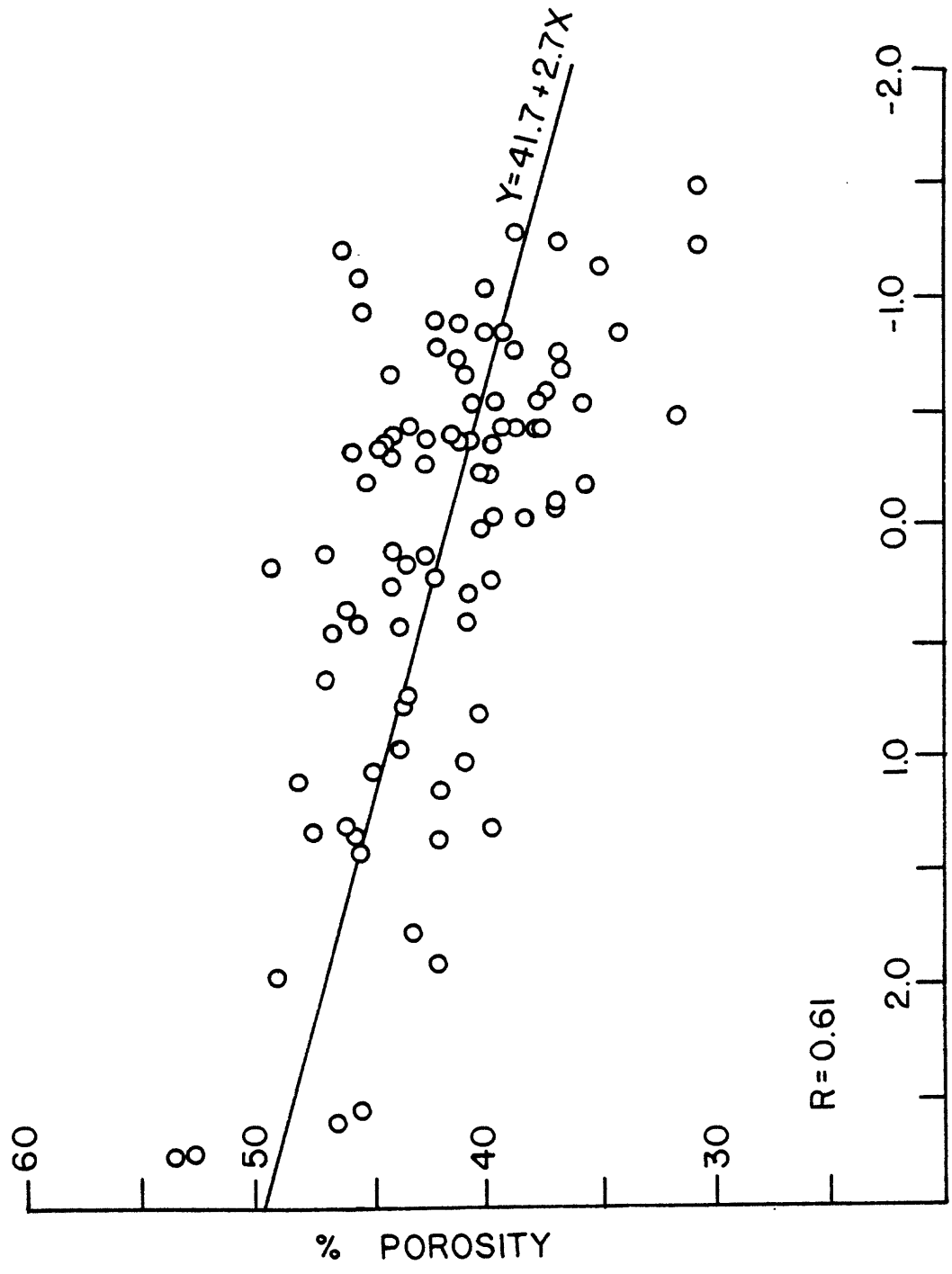

Figure 7. Mean grain size versus porosity. Data from both longitudinal bars on the South Platte River. For location of bar see Figure 2.

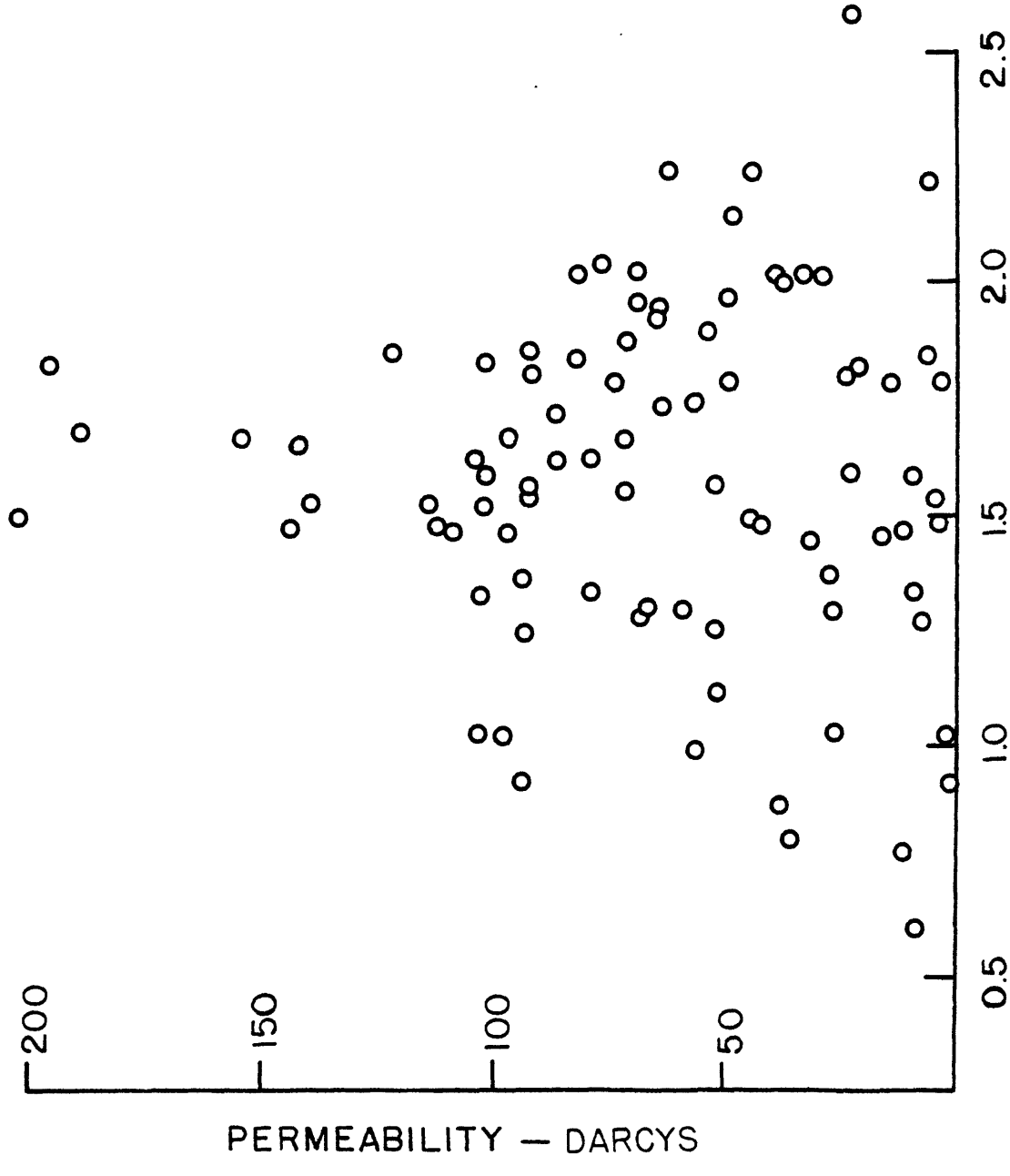

Figure 8. Sorting versus permeability. Data from both longitudinal bars on the South Platte River. For location of bars see Figure 2.

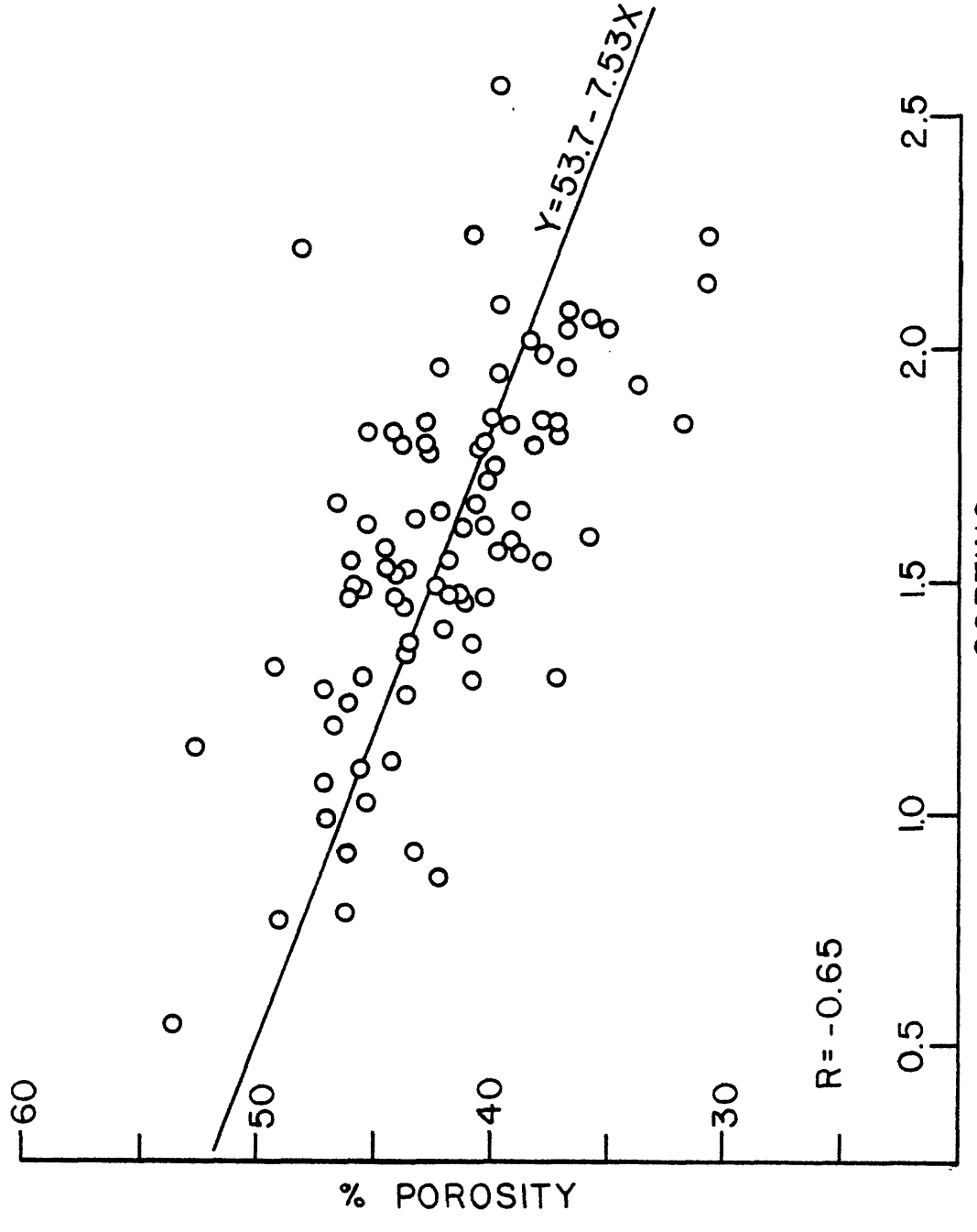

Figure 9. Sorting versus porosity. Data from both longitudinal bars on South Platte River. For location of bars see Figure 2.

Table 3. Relations of permeability and porosity to textural parameters: longitudinal bar and point bar sand bodies and experimental data.

	Point Bars[a]		Experimental Data I[b]		Experimental Data II[c]		Longitudinal Bars	
	Permeability	Porosity	Permeability	Porosity	Permeability	Porosity	Permeability	Porosity
GRAIN SIZE INCREASE	Increase	Increase	Increase	Decrease	Increase	Independent	Increase	Decrease
SORTING INCREASE	Increase	Increase	Decrease	Increase	Increase	Increase	Independent	Increase

[a] data from Pryor (1973)

[b] data from Fraser (1935)

[c] data from Beard & Weyl (1973)

of packing in natural sand bodies probably caused the deviations from the ideal models. The only experimental data available to Pryor, however, was that of Frazer (1935) (Table 3). Frazer's data do not take into account the relations between grain size and sorting and their affect on the ideal models. Beard and Weyl (1973) do take the relations into account and provide a complete range of permeabilities and porosities for various textural characteristics (Tables 4 and 5). When the ideal relations presented by Beard and Weyl (1973) are considered in conjunction with the grain size-sorting relation (Figure 10), the apparent discrepancies between the experimental data and the longitudinal bar data (Table 3) disappear. Beard and Weyl (1973) suggest that porosity is independent of grain size for a given sorting (Table 3 and Figure 4). It can clearly be seen, however, that as grain size increases sorting decreases in the longitudinal bar sand body (Figure 10). Under these conditions the ideal model (Table 4) predicts that as grain size increases, porosity will decrease and this is exactly what is shown by the data from the longitudinal bar sand body (Figure 7). The apparent discrepancy for the sorting versus permeability relations (Table 3) can also be explained by a similar examination of Table 5. Thus, the ideal relations between permeability-porosity and textural characteristics are demonstrated by naturally packed sands such as the longitudinal bar sand bodies. It therefore follows that permeabilities and porosities of unconsolidated sands can be estimated given data on textural characteristics (Table 4 and 5) as suggested by Beard and Weyl (1973).

Table 4. Porosities (percent) of artificially mixed dry-loose (L) and wet-packed (P) sand (after Beard and Weyl, 1973).

So	Size → / Sorting ↓	Coarse		Medium		Fine		Very Fine	
		Upper	Lower	Upper	Lower	Upper	Lower	Upper	Lower
1.0	Extremely well sorted	L 44.7 P 43.1	L 44.7 P 42.8	L 46.6 P 41.7	L 45.6 P 41.3	L 45.7 P 41.3	L 48.7 P 43.5	L 49.8 P 42.3	L 51.4 P 43.0
1.1	Very well sorted	L 42.7 P 40.8	L 44.1 P 41.5	L 44.3 P 40.2	L 43.9 P 40.2	L 44.8 P 39.8	L 47.5 P 40.8	L 49.6 P 41.2	L 51.8 P 41.8
1.2	Well sorted	L 41.2 P 38.0	L 43.7 P 38.4	L 42.5 P 38.1	L 43.9 P 38.8	L 44.7 P 39.1	L 46.0 P 39.7	L 49.5 P 40.2	L 51.9 P 39.8
1.4	Moderately sorted	L 37.4 P 32.4	L 37.6 P 33.3	L 39.4 P 34.2	L 41.0 P 34.9	L 41.9 P 33.9	L 44.1 P 34.3	L 48.1 P 35.6	L 52.6 P 33.1
2.0	Poorly sorted	L 33.5 P 27.1	L 34.9 P 29.8	L 36.4 P 31.5	L 38.0 P 31.3	L 41.8 P 30.4	L 47.3 P 31.0	L 52.7 P 30.5	L 57.0 P 34.2
2.7	Very poorly sorted	L 33.3 P 28.6	L 30.2 P 25.2	L 37.2 P 25.8	L 38.8 P 23.4	L 48.3 P 23.5	L 55.0 P 29.0	L 57.8 P 30.1	L 63.2 P 32.6
5.7		1.000	0.710	0.500	0.350	0.250	0.177	0.125	0.088 0.044

Median Diameter, mm

Table 5. Permeability (darcys) of artificially mixed and wet-packed sand (after Beard and Weyl, 1973).

So	Size → / Sorting ↓	Coarse		Medium		Fine		Very Fine		Average Adjusted (geometric mean) Permeability and Percent Error* for Upper Coarse Grain Size
		Upper	Lower	Upper	Lower	Upper	Lower	Upper	Lower	
1.0	Extremely well sorted	332[a] 475[b] 471[c]	221 238 236	106 119 118	71 59 59	33 30 29	15 15 15	3.1 7.4 7.4	3.8 3.7 3.7	475 ± 20
1.1	Very well sorted	434 458 376	225 239 133	113 115 94	53 57 48	34 29 23	15 14 12	6.7 7.2 5.9	3.5 3.6 2.9	458 ± 10
1.2	Well sorted	262 302 275	133 151 138	84 76 69	45 38 34	24 19 17	10 9.4 8.7	4.6 4.7 4.3	1.7 2.4 2.1	302 ± 20
1.4	Moderately sorted	79 110 137	50 55 68	32 28 34	16 14 18	7.0 7.0 3.6	3.6 3.5 4.3	0.87 2.1	0.16 1.1	110 ± 20
2.0	Poorly sorted	25 45 59	22 23 30	12 12 15	5.2 6.0 7.4	0.92 3.7	0.26 1.9	0.05 0.93	0.03 0.46	45 ± 5
2.7	Very poorly sorted	13 14 13	6.7 7.0 6.6	3.6 3.5 3.3	0.20 1.7	0.03 0.33	0.04 0.42	ND 0.21	0.02 0.10	14 ± 5
5.7		1.000	0.710	0.500	0.350	0.250	0.177	0.125	0.083 0.062	

Median Diameter, mm

So - Sorting coefficient (Trask)

The reproducibility of experimental permeability data in this portion of the diagram is poor, owing to difficulties in obtaining homogeneous packing. These data, therefore, are not considered in calculating average adjusted permeability values.

332[a] —experimental data for artificially mixed and wet-packed sand.
475[b] —average adjusted permeability computed from the experimental data.
471[c] —permeability computed at 40 percent porosity (Krumbein and Monk).

*Percent error was calculated from the antilog of the standard deviation of logarithms of the adjusted experimental permeability.

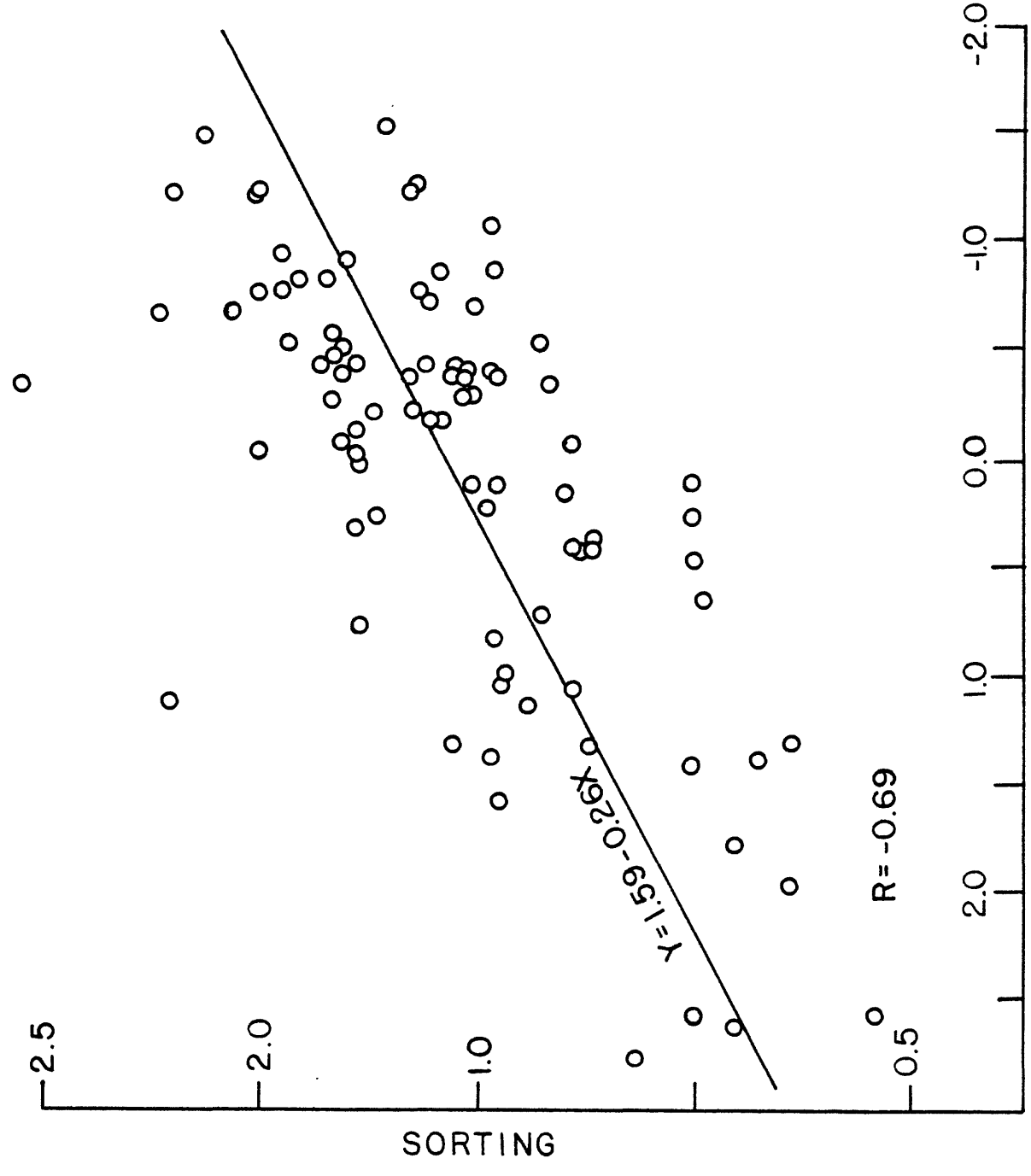

Figure 10. Grain size versus sorting. Data from both longitudinal bars on the South Platte River. For location of bars see Figure 2.

ANCIENT RIVER DEPOSITS - COLORADO PLATEAU

In addition to the field work on modern river deposits described in the previous section, a portion of the project effort has been and continues to be a field investigation of the sedimentology and contained uranium deposits in the Colorado Plateau. In particular, field trips have been made to both the Grants and the Uravan mineral belts in New Mexico and in Colorado (Figure 11) and detailed investigations are underway in the Slick Rock District of the Uravan mineral belt.

Most geologists who have investigated the sedimentological characteristics of the Westwater Canyon Member of the Morrison Formation in the Grants mineral belt have concluded that this unit (the main ore-bearing unit) consists of a coalesced sequence of braided stream deposits (Criag, et al., 1965; Campbell, 1976; Rackley, 1976; Green and Pierson, 1977; Huffman and Lupe, 1977; Galloway, 1978; Young, 1978; Falkowski, 1979; and others). We have observed the vertical succession of sedimentary structures and grain size and concur with this interpretation. Many of these same investigators also suggest that the braided stream deposits of the Westwater Canyon were part of a large, low gradient, wet alluvial fan, based largely on the paleocurrent directions and sandstone isolith patterns (Figure 12). Turner-Peterson (1980) disputes this contention and suggests that the Westwater Canyon was deposited as a braided alluvial plain. She contends that the fan shape pattern shown in Figure 12 results from the lumping of lower Westwater Canyon sediments, which have a predominantly northeast orientation, with upper Westwater Canyon sediments, which have a more uniformly southeast orientation (Saucier, 1976).

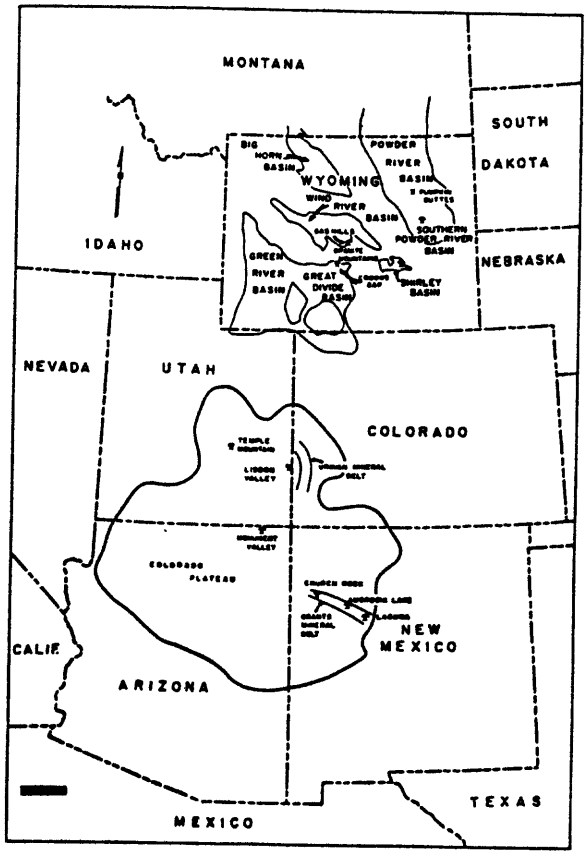

Figure 11. Uranium mineral belts of the Colorado Plateau and Wyoming (after Rackley, 1976, p. 90). Black bar in lower left of map is 62.1 mi. (100 km) in length.

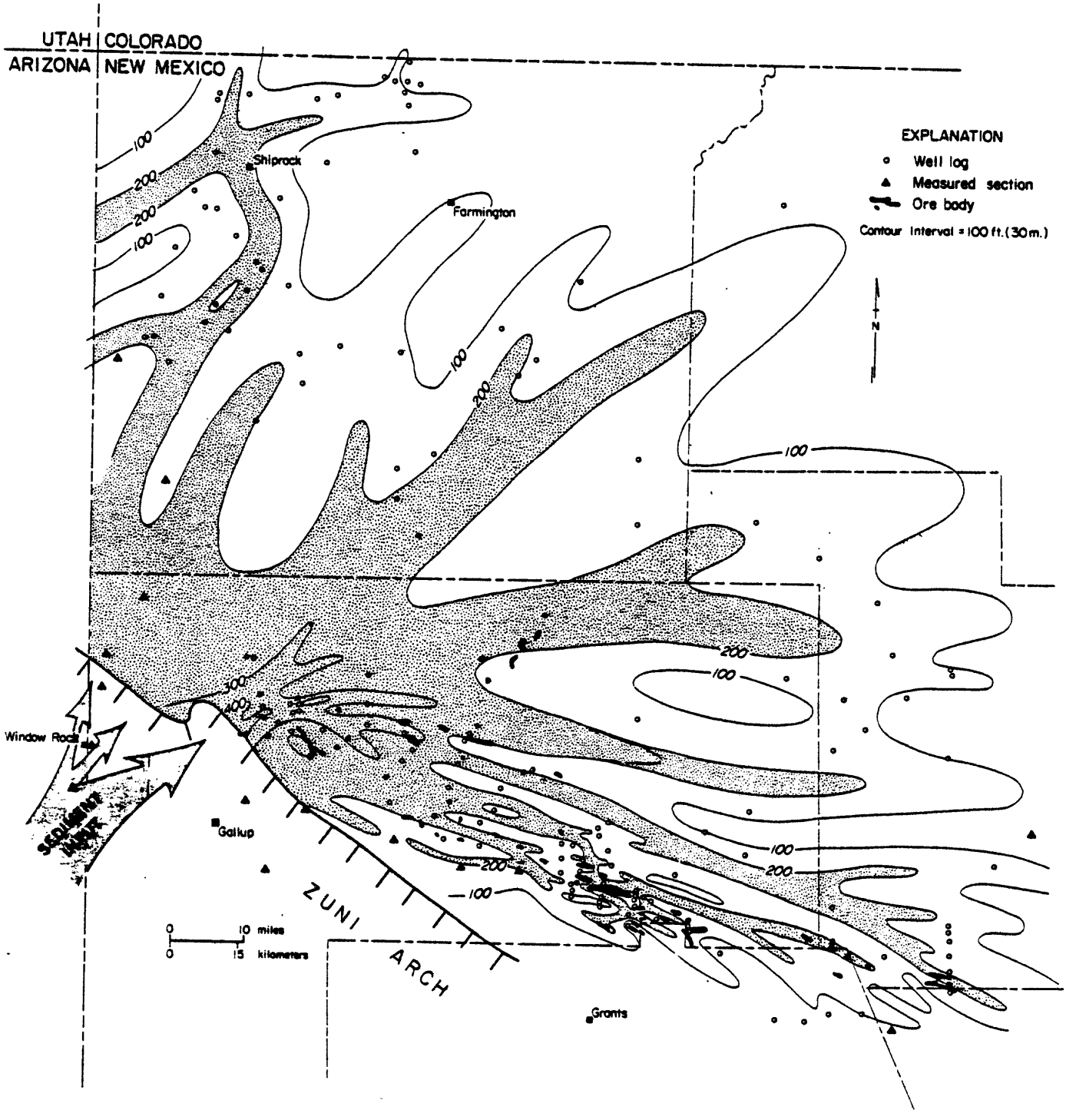

Figure 12. Sandstone isolith map of the Westwater fan system based on outcrop sections and subsurface log data (after Galloway, 1978).

Within the mineral belt the bulk of the Westwater Canyon deposits consist of trough cross-bedded sheet sandstones which constitute a sheet-like sandstone body. Internally, this sandstone contains large scale "channel systems" and small scale channel fill deposits (Campbell, 1976). Four types of channel-fill deposits recognized by Galloway (1978) include: braided bedload channels, straight bedload channels, sinuous mixed-load channels, and distributary mixed-load channels. These four types of channel-fill deposits are distinguished on the basis of grain size and the relative importance and vertical distribution of sedimentary structures; including trough cross-beds, horizontal beds, and planar cross-beds (accretionary beds of Galloway, 1978). As previously discussed these three sedimentary structures are also common in Holocene Platte River deposits. Minor amounts of climbing ripple laminations and deformed bedding are present in the more distal channel-fill deposits (the distributary mixed-load channels). The source area for the sediments of the Westwater Canyon was southwest of the Grants mineral belt. The proximal deposits of this fluvial system have been truncated by post-Jurassic erosion (Craig, et al., 1955; Saucier, 1976; Galloway, 1978; and others).

The sedimentologic characteristics of the Salt Wash Member of the Morrison Formation in parts of Arizona, New Mexico, Colorado and Utah has been examined by numerous individuals since the early 1940's. It has long been recognized that the Salt Wash was the product of fluvial deposition (Stokes, 1944). It is, however, our contention that the nature and specific environments of this ancient river system have never been adequately described and furthermore that many false assumptions regarding Salt Wash deposition are engrained in the modern literature. One early

investigation, generally ignored in subsequent studies is that of Stokes (1954). Stokes examined the Salt Wash in several widely spaced areas in southeastern and northeastern Utah. One of these areas was the Blanding district just west of the current study in the Slick Rock district. Stokes described the Salt Wash as a fluvial accumulation on a wide aggrading flood plain. While he did not specifically state that the Salt Wash was the product of a meandering stream system, he suggested this possibility in his maps of sedimentary trends (Figure 13) and in his discussion of the favorable sites for ore mineralization (e.g. such favorable sites are thought to be mainly old river bends which are shown by curving patterns of sediments; Stokes, 1954, page 5. Two regional stratigraphic studies of the Salt Wash which succeeded Stokes' 1954 study have received much broader acceptance in the literature (Craig, et al., 1955 and Mullens and Freeman, 1957). In both studies it was concluded that the preserved Salt Wash constitutes a fan shaped wedge of sedimentary rocks with its apex in south-central Utah (Figure 14). Based on this geometry, paleocurrent trends and the general internal character of the sediments it was suggested that the Salt Wash was deposited by an aggrading distributary system of braided channels on a fan shaped alluvial plain or alluvial fan. This interpretation of the Salt Wash depositional system has been accepted by most subsequent investigators and has been applied to the deposits in the Uravan mineral belt (Shawe, 1962; Motica, 1968; Rackley, 1976; Young, 1978; and others). Results of detailed field investigations in the Slick Rock District of the Uravan mineral belt dispute this generally accepted interpretation. These investigations led us to suggest that the Salt Wash Member, including the so-called uraniferous upper ledge, was deposited in a meandering river system (Tyler and Ethridge, in press).

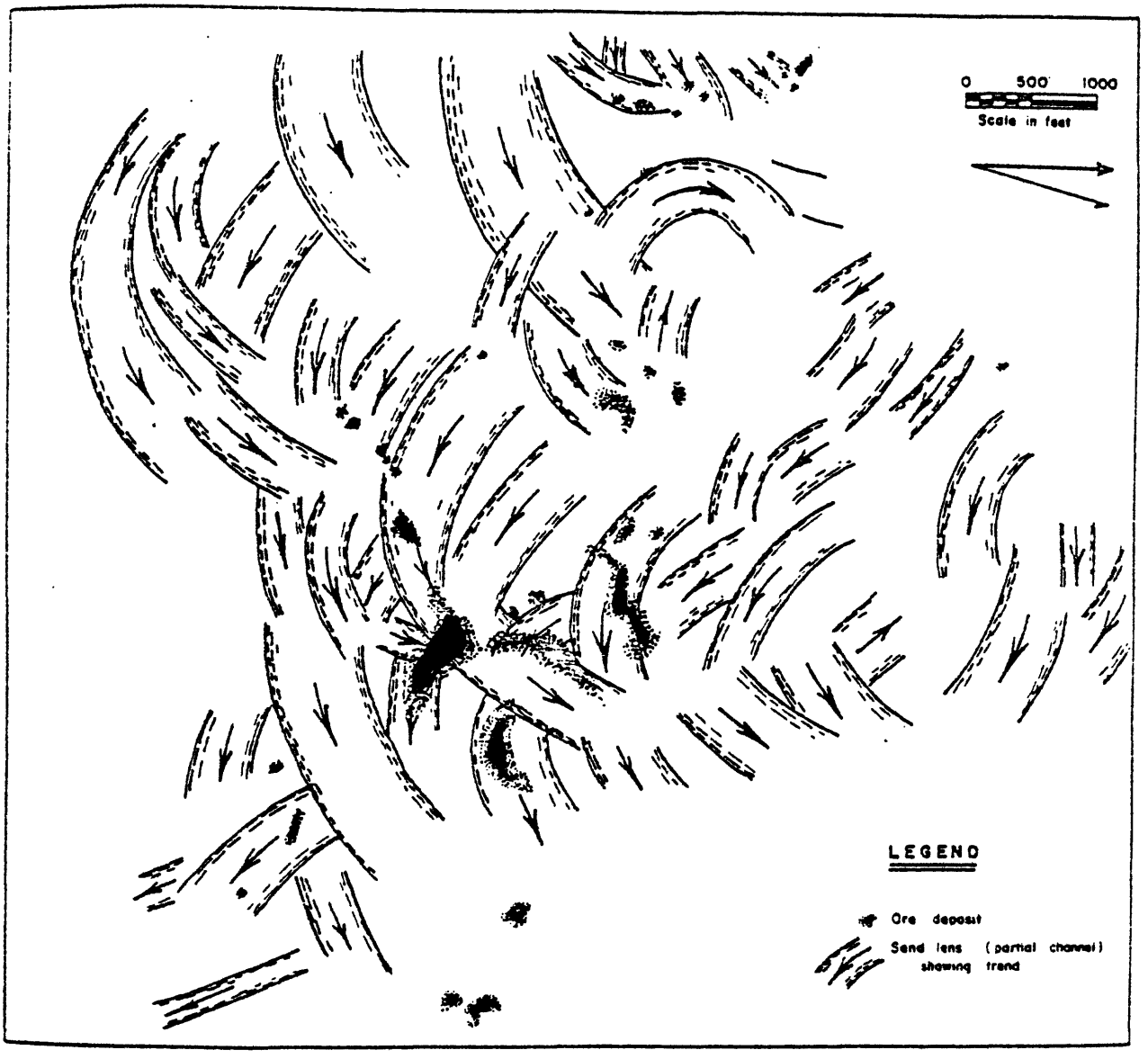

Figure 13. Sedimentary trends and ore body locations in the vicinity of the Blanding Mines, San Juan County, Utah (from Stokes, 1954, p. 45, Figure 21).

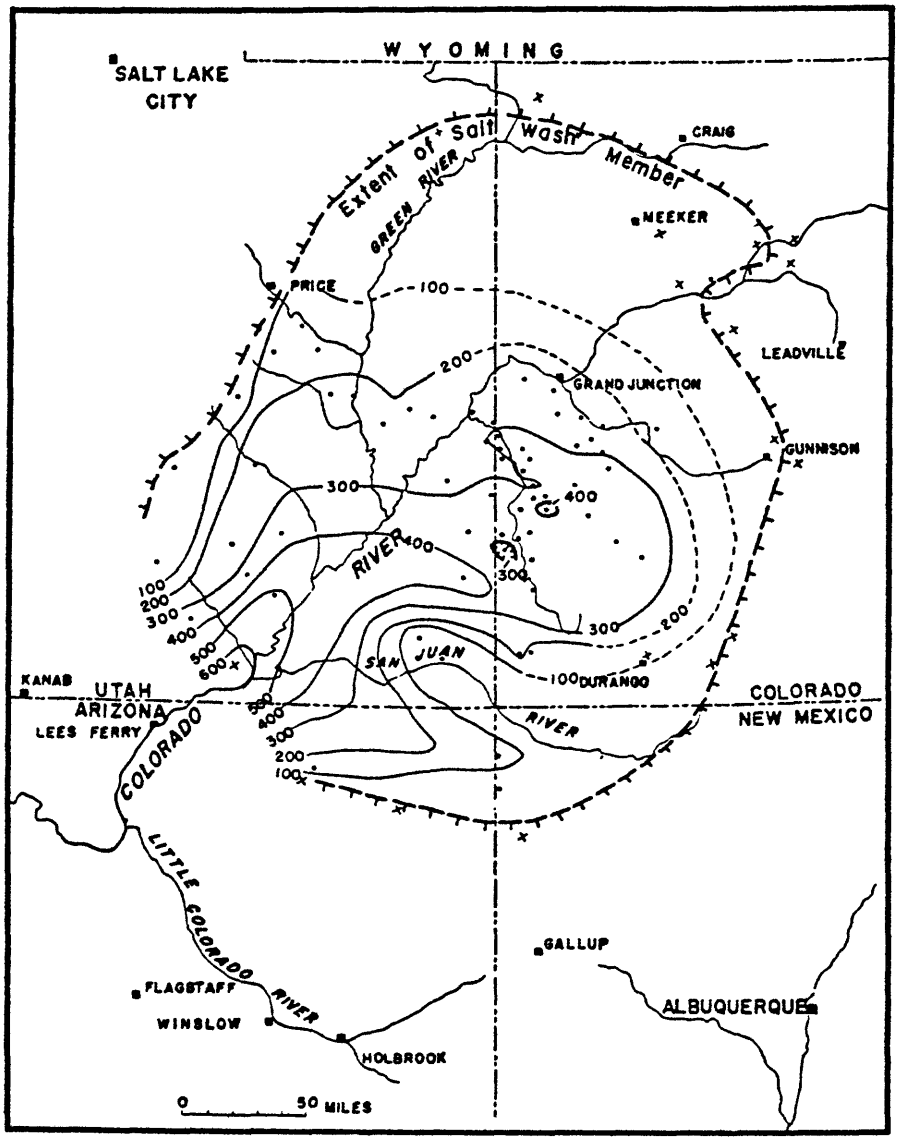

EXPLANATION

• Lithofacies Locality

—100— Isopach Line, Dashed Where Inferred

× One Measured Section

Extent of Salt Wash Member

Isopach Interval 100 Feet

Figure 14. Isopach map of Salt Wash Member of Morrison Formation (from Mullens and Freeman, 1957, p. 512, Figure 4).

Since fine-grained meander belt systems are not usually associated with alluvial fan systems, it is unlikely that the Salt Wash was deposited on an alluvial fan. It is, of course, still conceivable that the Salt Wash west and south of the Uravan mineral belt was deposited as an alluvial fan system. At this time in our study we made no attempt to speculate on the environment(s) of the Salt Wash outside of the immediate study area in southwest Colorado.

Unlike the previous investigations, which relied heavily on gross geometry of the sediments and generalized vertical and lateral relations between sandstone and mudstone (or siltstone) units, this study was designed to investigate the detailed character of sedimentary structures and lateral and vertical relations displayed by these structures and the average grain size. To date, 30 detailed vertical profiles have been measured through part of the Salt Wash and the underlying Summerville Formation. In addition, generalized descriptions have been made of underground mine walls in four different mines throughout the mineral belt. One of the more important observations made about the nature of the measured sections is that the Salt Wash consists of up to 54% fine-grained bioturbated and/or rooted mudstones and siltstones with thin discontinuous sandstone lenses (Figure 16, Section 16, 90-100 M). These fine-grained sediments are interstratified with thicker sandstone units (Figures 15 and 16). The fine-grained sediments have many of the same characteristics described by Reading (1978) for Recent and ancient floodplain sequences. Most previous investigators have also recognized these fine-grained units as floodplain deposits. The discontinuous sandstone lenses within these fine-grained sequences probably represent flood deposits known as overbank and/or crevasse splays. Several

Figure 15. Detailed lithologic log of measured section No. 11, Slick Rock district, southwest Colorado. (from Ethridge, et al., 1980, Fig. 15)

SECTION No: 11 LOCATION: Slick Rock North

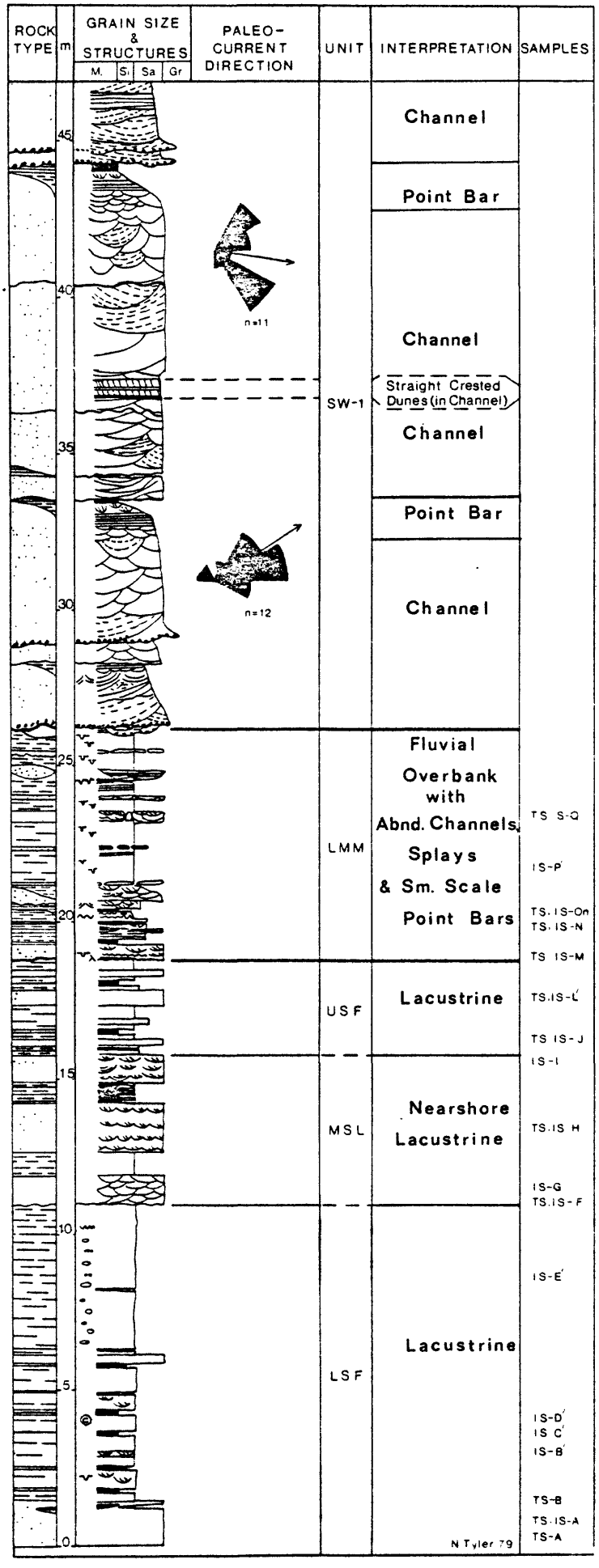

STRUCTURES

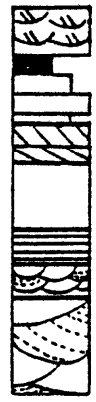

Ripple-trough crosslamination

Interbedded sandstone, siltstone and mudstone

Planar crossbedding

"Structureless" sand or siltstone

Horizontal lamination

Small scale

Large scale

Trough crossbedding

ROCK TYPE

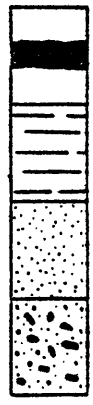

Mudstone

Siltstone

Sandstone

Conglomerate

CONTACTS

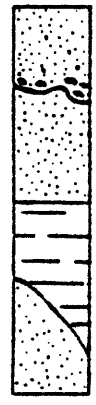

Erosional

Sharp

Gradational

ACCESSORIES

Mudcracks

Water-escape structure

Contorted beds

Limey nodules

Rooting

Burrows

UNIT DESIGNATION:

LSF- LOWER SUMMERVILLE FM.

MSL- MIDDLE SUMMERVILLE LEDGE

USF- UPPER SUMMERVILLE FM.

LMM- LOWER MORRISON MEMBER

SW-1 - FIRST SALT WASH LEDGE

LEGEND

Figure 16. Detailed lithologic logs of measured sections 15 and 16, Slick Rock district, Colorado.

SECTION 15 Bishop Canyon

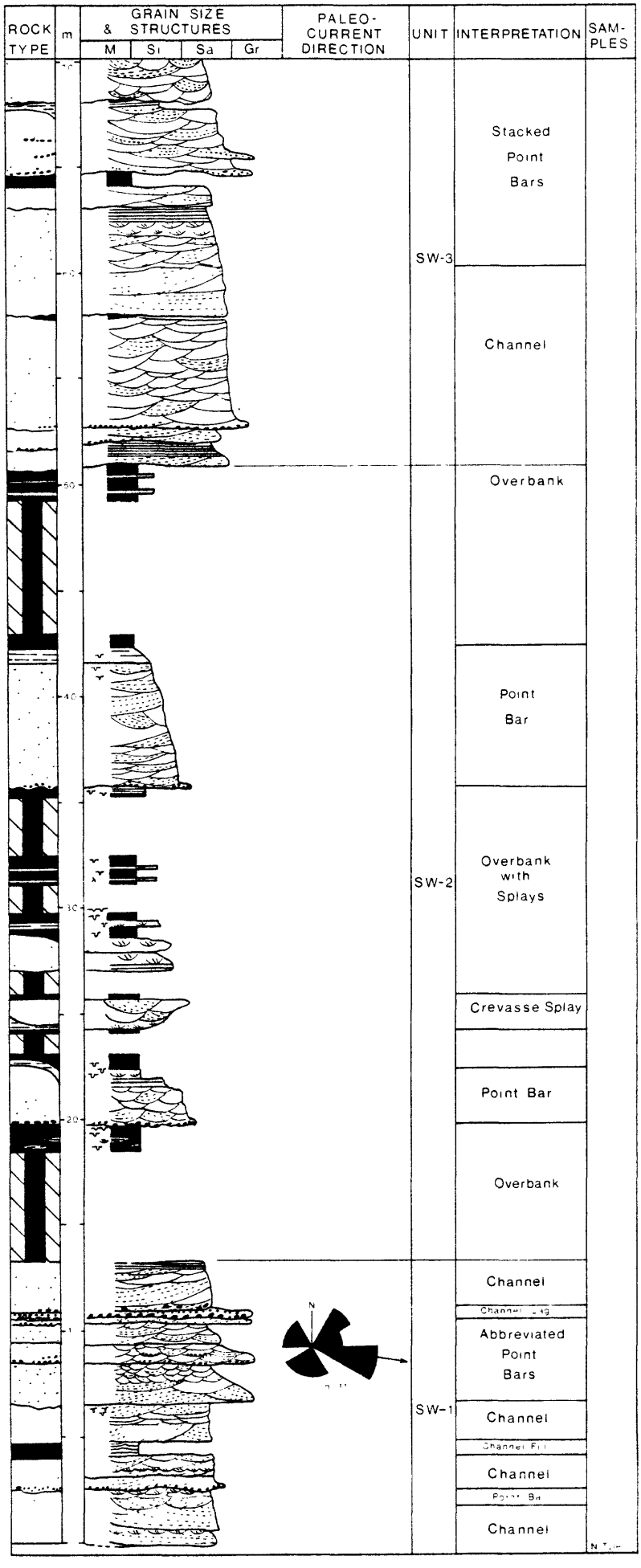

SECTION 16 Radium Mines Summit Canyon

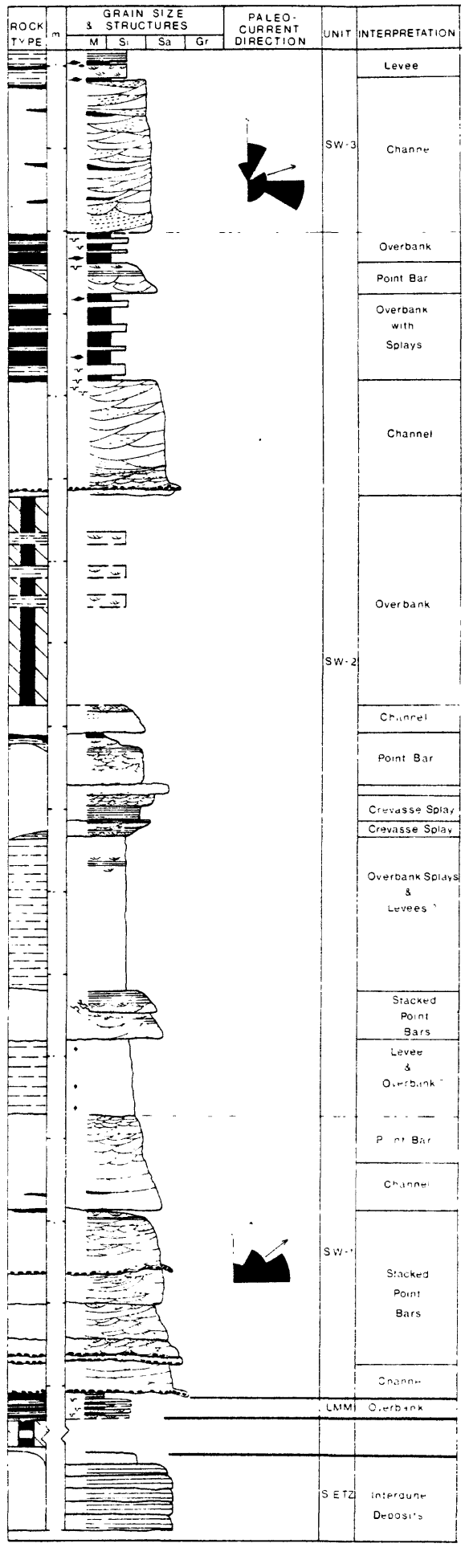

of the thicker splays reveal the typical coarsening and thickening upward sequence typical of crevasse splays (Elliott, 1974). These splays often have convex-up tops (Figure 17). The relatively high percentages of fine-grained overbank deposits and crevasse splay sandstones are more characteristic of meander belt systems than of braided alluvial or alluvial fan systems. The thicker interbedded sandstone units consist of two types of vertical sequences. The first type is the classic fining and thinning-upward point bar sequence. A complete point bar sequence consists, from bottom to top, of basal conglomerates often characterized by mudclasts, trough cross-bedded sandstone, horizontally laminated sandstones, and cross laminated (ripple-drift) sandstones (Figures 15 and 16). Upper contacts of these sequences are usually gradational into fine-grained overbank deposits. This now classic fining-upward sequence was first described by Bernard and Major (1963), refined and extended by Allen (1965 a and b; and others) and is reviewed by Reading (1978). The wide variability in crossbed directions from bed to bed and between ledges within the study area is more typical of meandering stream than of braided stream deposits. Furthermore, the wide variation in paleocurrent directions does not fit in well with the simple arcuate regional paleocurrent patterns presented by Fischer and Hilpert (1952) and Craig, et al., (1955).

The second type of sequence is characterized by abundant large-scale, low angle, trough crossbedded, medium-grained sandstones (Figures 15 and 16). Local mudstone lenses occur throughout these sandstone units. Logs, bone beds, and basal mud clast conglomerates are common. Basal contacts are sharp and erosional and upper contacts are sharp and occasionally gradational. These sequences are similar to the mixed-load/bed-load channel

A

B

Figure 17 (A) Overall view of crevasse splay deposit, Salt Wash Member Morrison Formation Slick Rock District. Note Convex up outline of top of deposit. (B) Close up view of A showing thickening upward sequence of sedimentary structures.

facies (Galloway, 1978) which were presumably deposited in broad, low sinuosity, laterally migrating channels.

In the study area the sandstone units interpreted as point bar and channel deposits occupy a series of discontinuous ledges numbering between 3 and 6. Each ledge consists of a number of complete or abbreviated sequences that range from a few feet to 25 feet in thickness. Sandstone units grade laterally and vertically into ripple laminated and rooted levee, fine-grained abandoned channel-fill, and crevasse splay deposits. Cross bed directions show a wide variation between beds and between ledges (Figures 15 and 16) which is more typical of meandering stream than of braided stream deposits.

The fluvial architecture (geometry and internal arrangement of channel and overbank deposits; Miall, 1978, p. 33) is currently under investigation. This investigation involves the description and correlation of subsurface cores, geophysical logs and drillers logs and the integration of this data with surface data (measured sections) and data presented in Shawe (1968).

The preliminary results of the examination of the relative proportions of sandstone versus mudstone and channel versus point bar deposits for the entire Salt Wash member suggests two major sandstone belts that may represent trunk streams that traversed the Slick Rock district in a general west to east direction (Figure 18). These areas are characterized by a higher percentage of sandstone and by a greater abundance of channel deposits. Areas adjacent to the sand belts have lower sand-shale ratios and are characterized by a greater abundance of point bar deposits. This information, coupled with paleocurrent patterns, suggests that the high sand areas

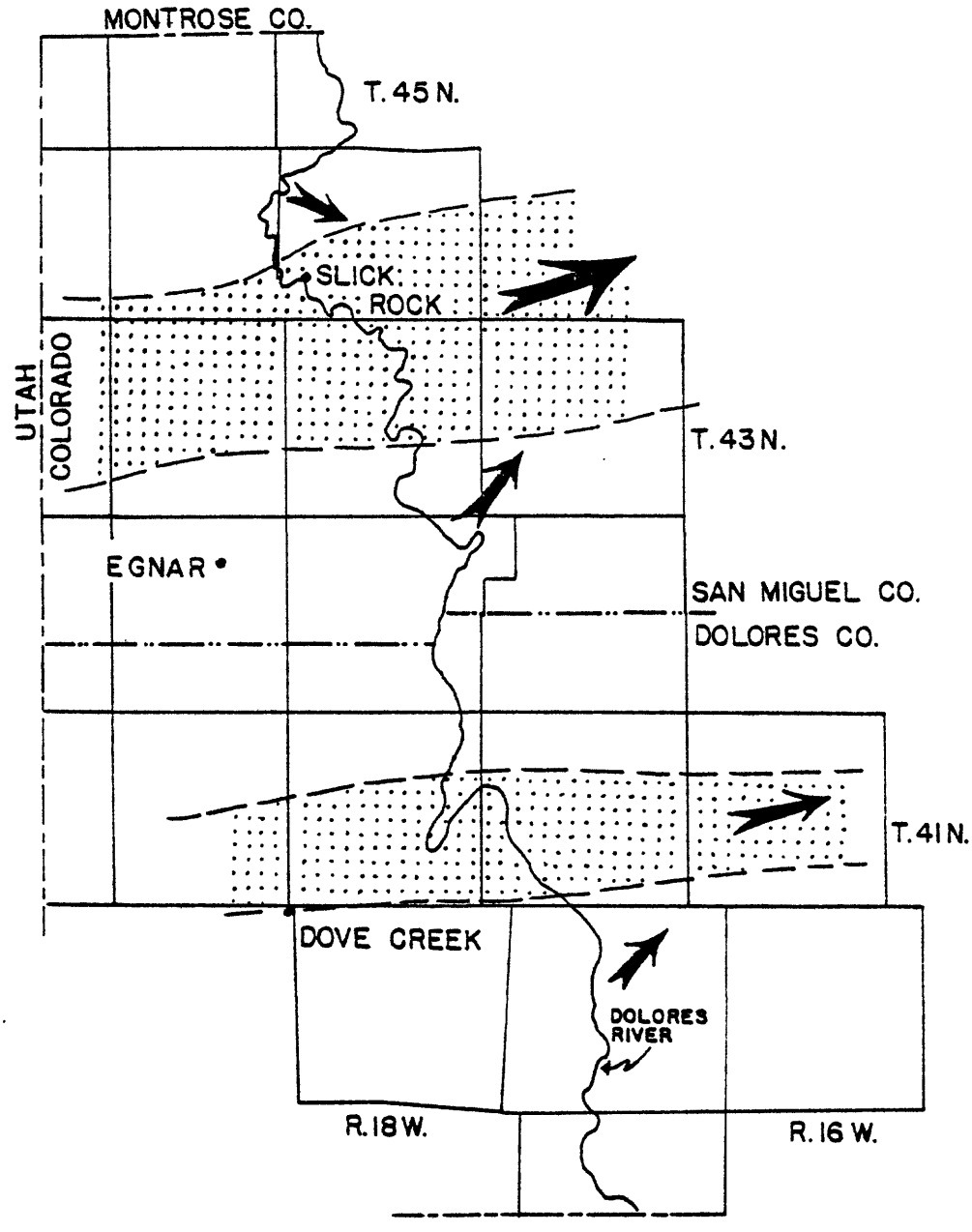

Figure 18. Generalized and inferred patterns of major trunk streams (major axes of sand deposition) and tributary subsystems, Salt Wash Member, Morrison Formation, Slick Rock district, southwest Colorado. Areas with stippled pattern have sand/shale ratios high than 1 (Data and interpretation from work in progress by Noel Tyler and F. G. Ethridge).

represent principal fluvial axes of major trunk streams while the low sand areas constitute floodbasins traversed by tributary channels (Figure 18).

Because of the difficulty in defining the lower contact of the Salt Wash, our field studies have included an examination of the underlying Summerville Formation and the Junction Creek Sandstone. The Summerville Formation has been interpreted as a marginal marine and/or tidal-flat deposit (Shawe, 1962; Girdley, et al., 1975; and Young, 1978) and as lacustrine (Isachsen, et al., 1955).

The Summerville deposits consists of interbedded mudstones and siltstones which are laterally persistant over many hundreds of meters. Fine-grained sandstone occurs as thin beds within the mudstone and siltstone, but is most noticable as the resistant mid-Summerville ledge, a trough cross-bedded and ripple cross-laminated sandstone (Figure 15). This sandstone has abundant salt casts indicating periodic exposure and evaporation. The mid-Summerville ledge grades upwards into massive, laterally persistant interbedded muds and silts which are abruptly overlain by the overbank-fluvial sediments of the Lower Morrison Member.

The Summerville Formation rests upon terrestrial deposits (the eolian Entrada in the study area, and in southwestern Colorado the lacustrine Todilto limestone (Picard and High, 1972) and is overlain by terrestrial deposits (the Junction Creek Sandstone, and the Lower Morrison Member). Abundant shoreline deposits are lacking; rather, deposition of below wave base sediments and subsequent regression was followed abruptly by eolian or fluvial sedimentation. According to Picard and High (1972) this is characteristic of lacustrine sedimentation. The origin of the Summerville Formation remains problematical and further investigations are in progress.

Large-scale planar to wedge planar cross-bedding in the Junction Creek Sandstone, which outcrops in the southern part of the study area, suggests that this unit was deposited as an eolian dune complex that probably migrated across the surface of the dried up Summerville Lake. A similar origin for the Junction Creek sandstone has been proposed by Shawe, (1968) and Girdley, et al., (1975).

POROUS-MEDIA FLUME EXPERIMENTS

A. Description of the Physical Model

Laboratory experiments for this phase of the study were conducted in a small plexiglass flume containing a porous media. The flume is 3.0 feet (0.9 m) long, 12.0 inches (30.5 cm) high and 1.5 inches (3.8 cm) wide. A diagrammatic view of the porous-media flume is shown in Figure 19.

Humic acid and aluminum potassium sulfate solutions were used as the fluids in these experiments. In all experimental runs conducted during the second phase of this study, the porous-media model was first saturated with humic acid and the aluminum solution was then injected as a point or a dispersed source. Further details on the physical model as well as the solutions used are presented in a report covering the first phase of this study (Ortiz, et al., 1978)

Seven different types of porous media ranging from fine sands to glass beads were used to simulate different hydraulic properties. For any given run the flume was filled with a selected combination of porous media to simulate layered deposits. The hydraulic properties of the media used in these experiments are presented in Table 6.

B. Description of Experimental Run

The initial conditions for each porous media model test were those of a horizontal piezometric surface at a selected elevation higher than the top confining boundary. This was achieved by observing the piezometric head levels from a row of piezometers, located on one sidewall of the model, to ensure that no detectable hydraulic gradients existed.

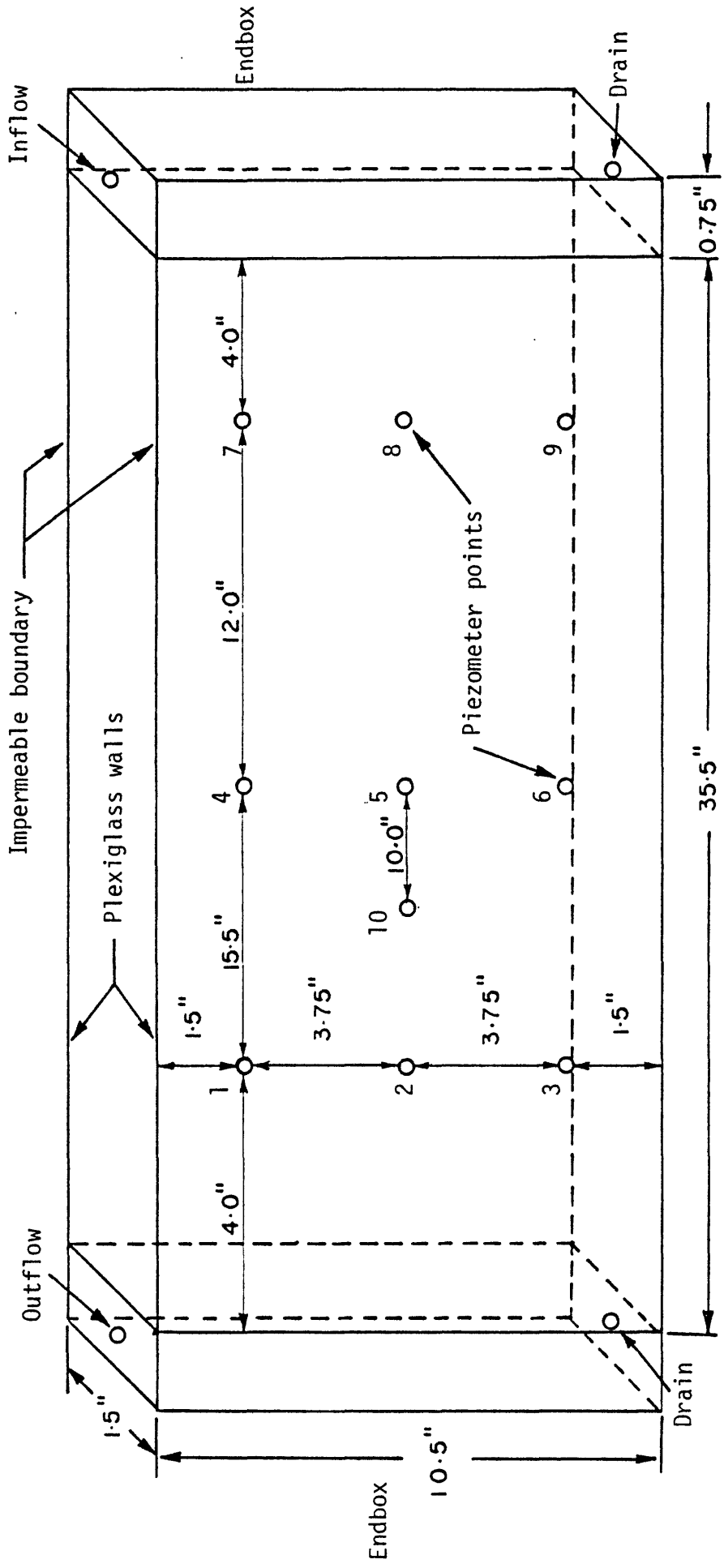

Figure 19. Diagrammatic view of small porous media flume used in experimental media flume used in experimental runs for Phase 2 of the study.

Table 6. Properties of Porous Media

Type	Hydraulic Conductivity (cm/sec)	Porosity	Grain Size (mm)	Description
Glass Beads	5.1	0.38	2.35	Spherical glass beads
Small Beads(E)	1.3	0.39	1.60	
Ottawa Sand(D)	0.65	0.33	0.5 -0.84	Ottawa sand
Fine Ottawa(C)	0.11	0.36	0.42-0.59	
Coarse	0.95	0.39	0.71-2.5	Coarse sand
Sand B	0.06	0.31	0.15-0.6	Fine sand
Sand A	0.01	0.36	0.15-0.3	Very fine sand

A constant flow rate of humic acid was then initiated at the upstream end of the model from the end box. At the same time a constant flow of aluminum potassium solution was injected as a point source through one of the piezometer openings located at the upstream end of the model. The positive displacement pump was used to introduce both fluids into the flume. During a test, changes in the flow and depositional pattern were recorded photographically at selected intervals of time. Data collected during each test included the piezometric head, inflow rate of each fluid, combined fluid outflow and a photographic record of flow configuration. The test was continued until no detectable changes in the flow configuration or precipitation band were observed.

Twenty-nine runs were conducted during the first and second phases of this study and are presented in Table 7. Only runs 3 and 19 to 29 are pertinent to the present discussion. The following conditions were studied:

1) Homogeneous porous medium, point recharge uniform discharge and no density difference between the fluids.
2) Simulated simple point bar deposit, point recharge, uniform discharge and no density difference between the fluids.
3) Simulated complex point bar deposit, point recharge, uniform discharge and no density difference between the fluids.
4) Same as 3, but with density difference.
5) Simulated complex braided stream deposit, point recharge, uniform discharge and no density difference between the fluids.
6) Same as 5, but with density difference.

Table 7. Summary of Experimental Runs

Run	Media	Boundary Conditions	Flow Rates (ml/min) Al	Flow Rates (ml/min) Humic	Test Duration (days)	Relative Fluid Densities	Injection Point	Solution Injected	Outflow Point	Outflow Head (cm)
Large Flume										
1	Homogeneous Ottawa Sand	Constant head upstream & downstream	0.0	not gaged	10.0	Equal	Top left tap	Hu	Bottom middle tap	-
2		Constant flow upstream - Constant head downstream	not gaged	not gaged	8.0	Equal		Hu	Downstream end box	-
Small Flume 1										
3			6.6	6.6	1.3	Equal	8	Al	Downstream end box	51
4	Rectangular Glass Bead Lens Centered in Ottawa Sand		0.92	0.15	3.0	Hu less	8	Hu	1	50
5			2.36	1.21	2.0	Hu less	8	Hu	Downstream end box	50
6		Constant flow upstream - Constant head downstream	2.68	0.39	3.0	Equal	5	Hu		50
7			4.27	2.15	1.8	Equal	9	Hu		50
8			5.15	2.57	2.0	Equal	9	Hu	1	50
9	Rectangular Sand A Lens Centered in Ottawa Sand		0.36	0.12	8.0	Al less	8	Hu	Downstream end box	50
10			7.85	2.74	0.9	Equal	8	Hu		50
11			7.79	2.59	1.0	Equal	8	Hu		50
12			1.06	0.38	5.0	Equal	5	Hu		50
13	30°,45° Medium Ottawa Sand with Baffles at Angles Indicated		8.17	2.69	2.0	Equal	8	Hu		50
14	30°,45°,45°		2.51	0.82	1.7	Equal	8	Hu		50
15	30°,45°,45°	Constant flow upstream - Constant head downstream	2.32	0.76	8.0	Equal	8	Hu		50
16	30°,15°,45°		4.27	1.36	2.0	Equal	8	Hu	Downstream end box	50
17	45°		8.5	8.6	1.2	Equal	10	Al		51
18	Layered:A,B,Ottawa & Coarse Sands; Two Mudstone Lenses		3.62	1.73	3.0	Equal	8	Hu		50
19	Multiple Layered: Fines Upward & Downstream; Simple River Deposits		1.19	2.31	5.0	Equal	2	Al		51
Small Flume 2										
20	Complex River Deposits: Baffles, Multiple Layers and Cross Bedding; Fines Upward and Downstream Simulation Point Bar Deposit		3.16	6.5	2.1	Equal	2	Al		50
21			3.8	11.7	1.8	Hu less	1	Al		50
22			0.57	1.72	10	Hu less	1	Al		50
23		Constant flow upstream - Constant head downstream	2.84	7.4	8	Al less	3	Al		50
24			0.3	0.0	30	Equal	10	Al	Downstream end box	50
25	Complex River Deposits: Baffles Multiple Layers, Foreset and Trough Crossbedding. Simulation Platte River Braided Stream Deposit		1.15	1.15	4	Hu less	2	Al		50
26			1.1	1.1	2	Al less	3	Al		50
27			2.1	2.1	9	Equal	1	Al		50
28		Constant flow upstream - Constant head downstream	2.0	2.0	4	Equal	Top	Al		50
29			0.5	0.0	20	Equal	5	Al	Downstream end box	50

C. Simulation of River Deposits

In an effort to examine relations between precipitate bands and enclosing sediments, information on the sedimentary structure, textural patterns, permeability and porosity of modern river deposits (Allen, 1965; Miall, 1978; and Pryor, 1973) were used to construct simple and complex fluvial deposit models in the porous-media flume. Both point bar and braided stream deposits were modeled.

For the simple point bar model five types of porous media were utilized to simulate textural differences and associated differences in porosity and permeability commonly found in point bar deposits. These materials included small glass beads, ottawa sand, fine-grained Ottawa sand, type B sand and type A sand (Table 6). The media grain size for this simulation was decreased both vertically and downstream (Figure 20). In the case of the complex point bar the same five media were used, along with mudstone lenses simulated by modeling clay. Greater lateral and vertical variability in terms of porosity and permeability differences were added and crossbedding was simulated by small scale layering of various combinations of porous-media materials (Figure 21). These complex relations more closely simulate actual point bar deposits described by Pryor (1973).

To simulate textural differences commonly found in braided stream deposits such as the Platte River (Smith, 1970 and Miall, 1978) three types of porous media were used. These materials include glass beads, Ottawa sand and fine-grained Ottawa sand (Table 6). This model consists of stacked planar crossbeds, and trough crossbeds and horizontal layers of small glass beads (Figure 22). Horizontal layers simulate longitudinal bar deposits while planar and trough crossbeds represent transverse bars

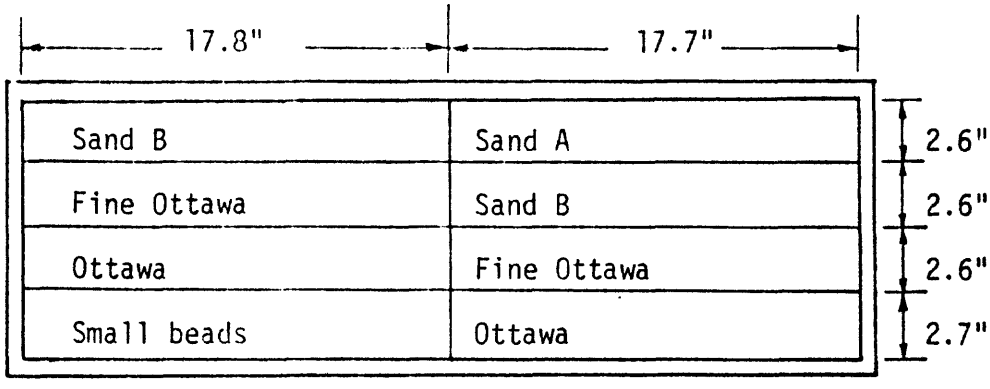

Run #19. River point bar

Figure 20. Simulation of simple point bar deposit.

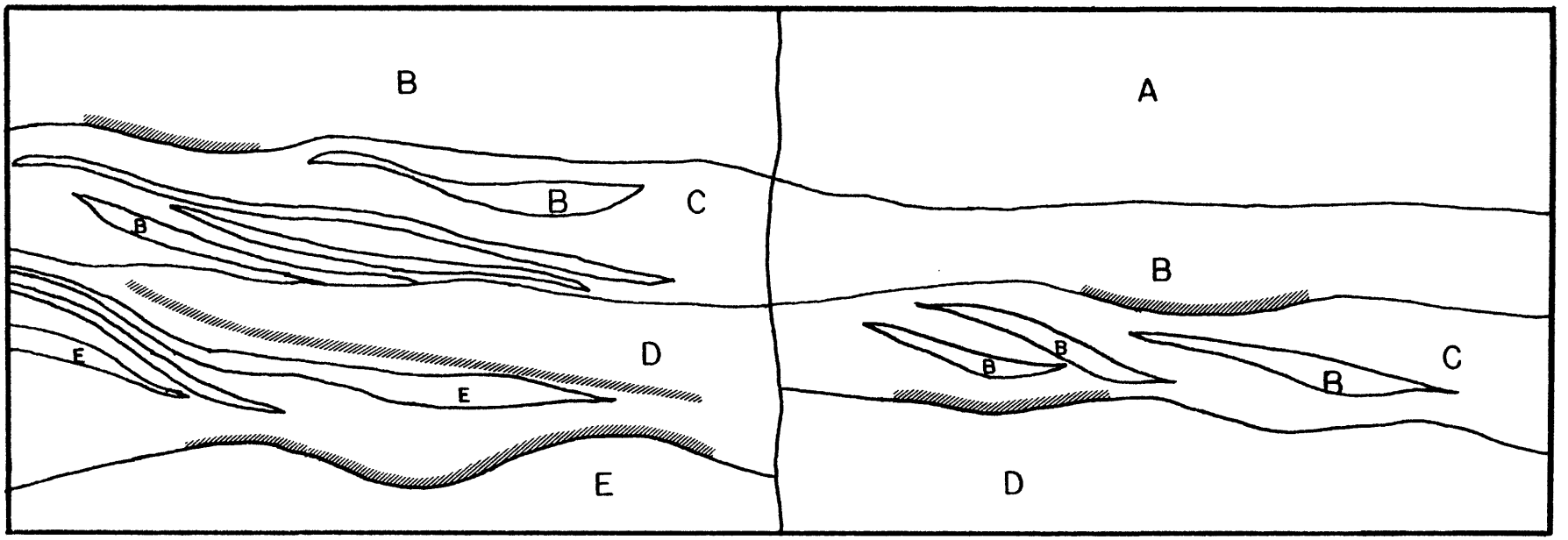

Figure 21. Cross section view of simulated complex point bar deposit in small porous media flume. Letters refer to different types of porous media as described in Table 6. Dimensions of flume are given in Figure 19.

and dune bed forms respectively (Miall, 1978). Mudstone lenses were simulated by modeling clay.

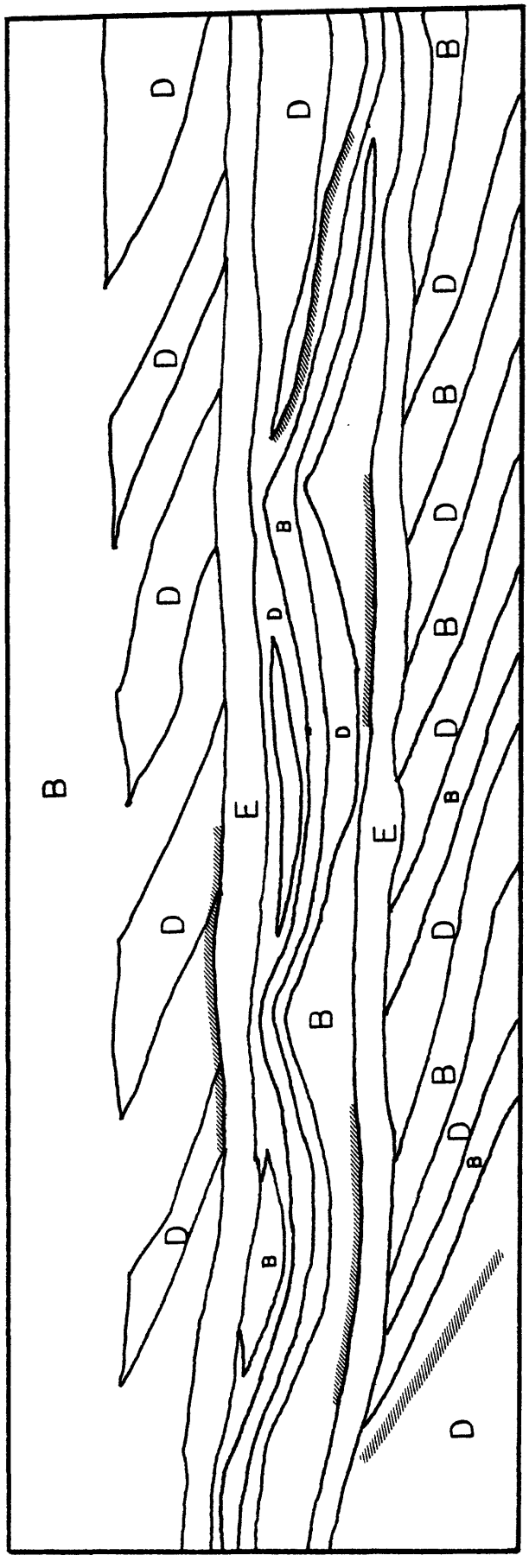

Figure 22. Cross section of simulated Platte River braided stream deposit in small porous media flume. Letters refer to different types of porous media described in Table 6. Dimensions of flume are given in Figure 19.

DISCUSSION OF EXPERIMENTAL RESULTS

In the second phase of this study emphasis was placed on examining the relationships between precipitate bands and enclosing sediments. This was accomplished by conducting a series of experimental runs in a porous media flume simulating point bar and braided stream deposits. In these runs the porous media model was saturated with humic acid and the aluminum solution was injected from a point or dispersed (Run 28, Table 7) source.

Details of the experiments involving the simulated simple and complex point bar deposits are presented in Table 7 (Runs 19 and 24). Experimental results for the simulated simple point bar model (Run 19, Table 7) indicate that the precipitate layer was denser in the coarser and more permeable material and became less dense in the finer and less permeable material. This was due primarily to the higher flow rates in the more permeable material, which provided more ions to react and precipitate for a given time period.

In the simulated complex point bar model (Runs 20-24, Table 7) the depositional processes were similar to those described above for the simple case, however, the patterns of precipitate bands are more complex owing to the greater lateral and vertical variability in porosity and permeability (Figure 23). Although in the laboratory experiments the precipitate was most pronounced in the more permeable layers, this may not always be the case under natural conditions. Different orders of magnitude between laboratory and natural flow rates and elapsed times may allow natural precipitates to form away from the more permeable beds. Furthermore,

Figure 23. (A) Small porous media flume showing the effects of mudstone layers and complex porous media layering and cross lamination on the distribution of precipitate bands; Complex point bar model. Note the offset precipitate band across simulated mudstone lens at point X and the effect of simulated cross lamination at Y. General flow direction indicated by large arrow

(B) Small scale porous media flume showing effects of mudstone lenses and complex porous media layering on the shape and distribution of precipitate band; Complex point bar model. Note offsetting of precipitate band across simulated mudstone layer at point X and effects of mudstone lense at Y on the shape of the precipitate band. General flow direction indicated by large arrow.

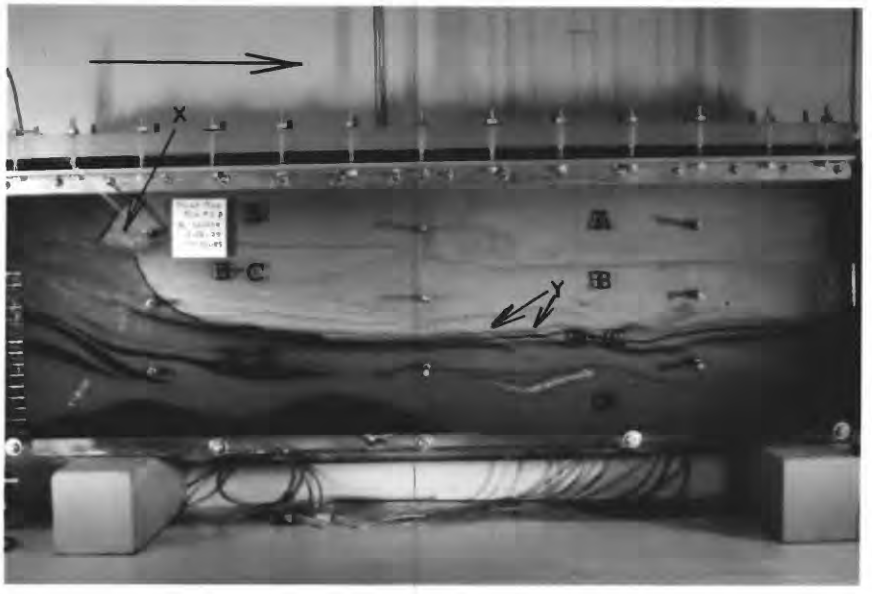

A

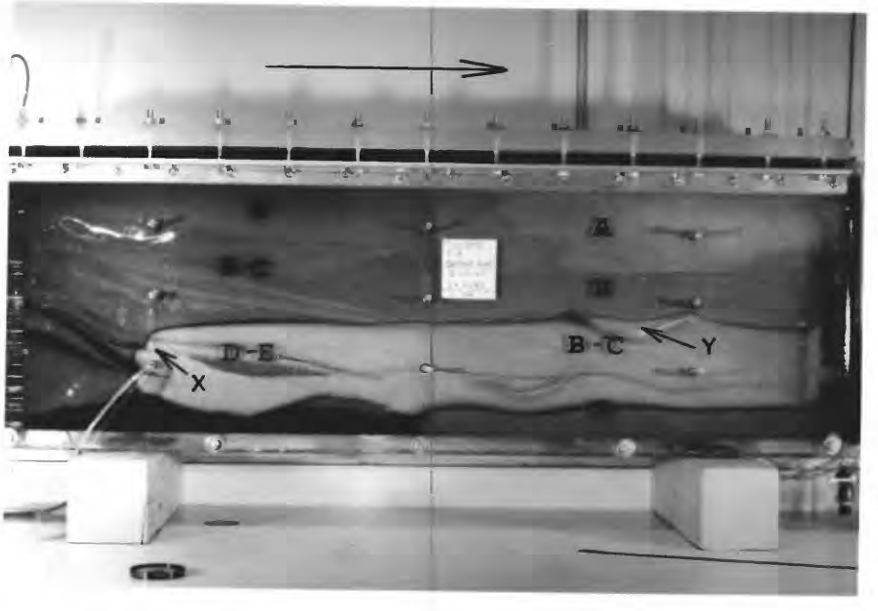

B

subsequent dissolution of precipitates resulting from the flow of later fluids might proceed more rapidly in permeable layers leaving remnants and pods in the less permeable layers.

Details of the experiments involving the simulated braided stream deposits are presented in Table 7 (Runs 25 to 29). In general, at the early stages of the experiment where non-steady state conditions prevailed, most of the flow of the aluminum solution, injected from a point source was channeled through the more permeable, coarser-grained horizontal layers of glass beads. The interface, therefore, was located temporarily in these permeable layers. It was apparent that the contact time between the two solutions was long enough to allow the fluids to react at the transient interface since a precipitate band was developed in these permeable layers (Figure 24A). These precipitate bands were preserved throughout the remainder of the experiment since the pH of the encroaching solution was not high enough to cause the precipitate to dissolve. As the flow approached steady state conditions the resulting precipitate bands became very irregular, developing almost a stair step topography related to the difference in hydraulic conductivity within adjacent cross-bed layers (Figure 24B) and to the directional permeability gradients that tend to parallel these inclined layers (Pryor, 1973 and Figure 1 this report) despite the uniform discharge from the downstream end of the porous-media flume. The influence of this directional permeability in the cross-stratified units, on the fluid flow patterns and the resulting precipitate band are clearly demonstrated in a 16 mm time lapse movie of Run 28. In this run the aluminum solution was injected from the top of the porous-media flume. Initial flow paths were down the inclined layers of the upper set of planar cross-beds and flow velocities were noticeably faster in the more permeable layers.

Figure 24. (A) Small-scale porous-media flume showing effects of cross laminations, horizontal beds, and mudstone lenses on the shape and distribution of precipitate bands; Braided stream model (Run 25 Table 7). Note the precipitate bands in both permeable horizontal beds and the effect of direction permeability gradients in upper zone of planar cross laminations. General flow direction indicated by large arrow.

(B) Small-scale porous-media flume showing effects of cross laminations, horizontal beds, and mudstone lenses on the shape and distribution of precipitate bands; braided stream model (Run 26, Table 7). Note the stable pocket of humic acid in the flow field of aluminum solution at point X, the aluminum pocket surrounded by humic solution at point Y, the effects of intertonguing of precipitate bands near the recharge area to the left and the effects of direction permeability in the cross laminated layers on the distribution of precipitate bands. General flow direction indicated by large arrow.

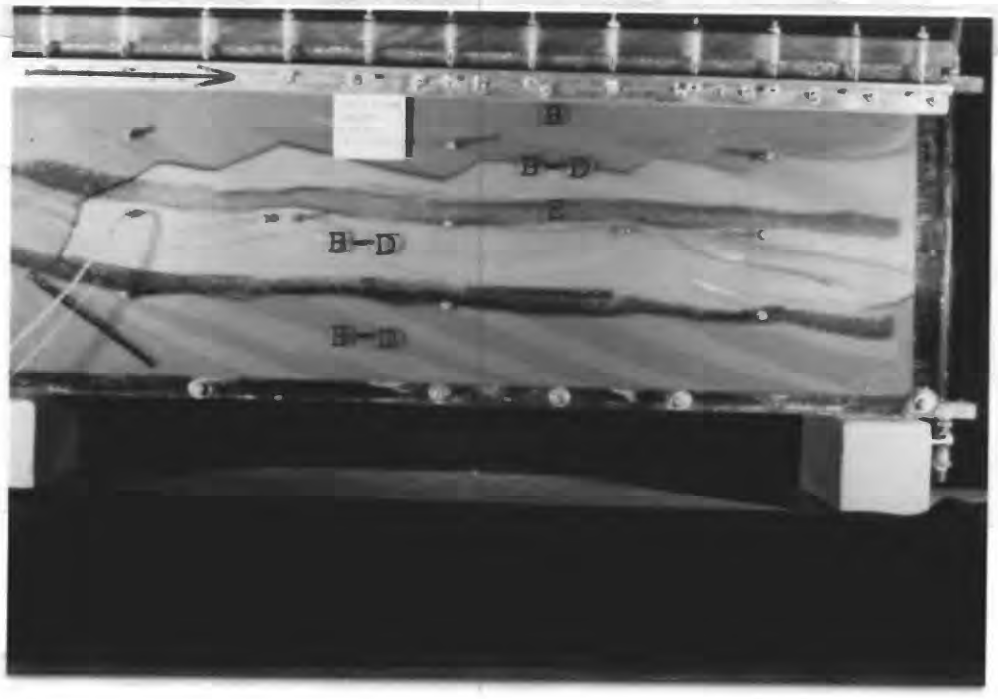

A

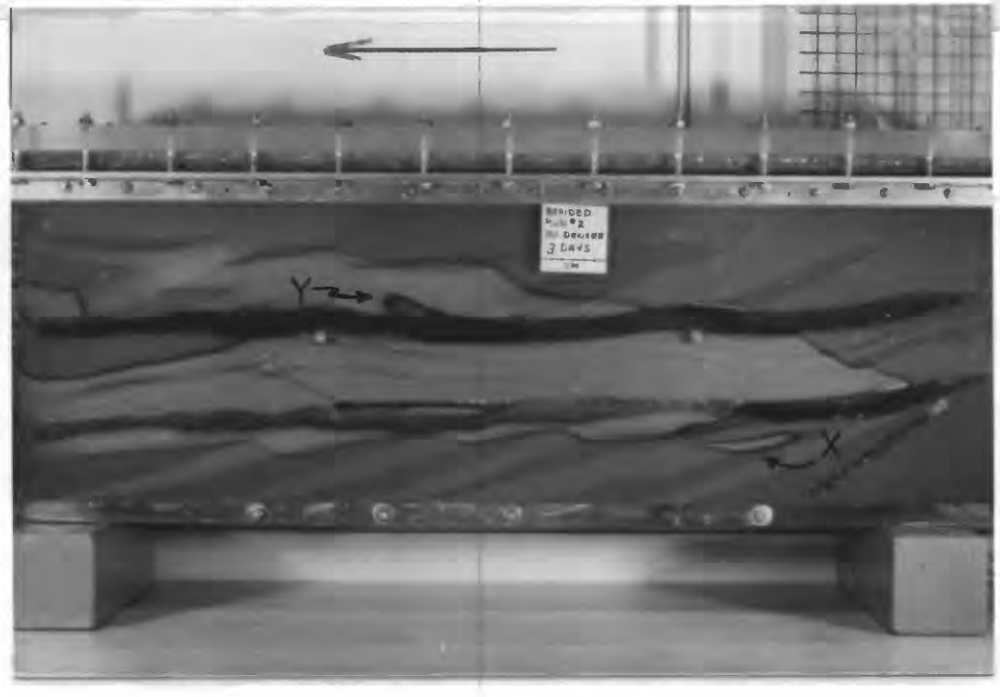

B

In Run 26 (Table 7), the aluminum solution injected from piezometer opening #3, was the less dense of the two fluids. Density differences caused the interface to rise as it traversed the flume. These differences in density, however, did not change the relative precipitate concentrations or the width and sharpness of the precipitate bands. Experimental results showed a stable pocket of humic acid in the flow field of the aluminum solution (Figure 24B). Similar remnant ore bodies completely encased in oxidized tongues are reported from roll type ore deposits (Granger and Warren, 1979). It is not known if similar deposits are found associated with the trend ore bodies of the Colorado Plateau.

Conversely, an aluminum pocket surrounded by humic acid was also observed (Figure 24B) near the injection point for the aluminum solution. The rapid initial expansion of the interface in the vicinity of the injection point, coupled with the subsequent rise of this interface due to density differences, and the permeability reducing characteristics of the precipitate may have resulted in the development of this isolated pocket of aluminum solution.

In the experimental studies conducted to date, numerous small-scale details in the relation between the precipitate band and the modeled sedimentary features are similar to relations between ore deposits and associated sedimentary structures in the Colorado Plateau deposits. Furthermore, these relations can be explained in terms of permeability, porosity, textural, and sedimentary structure patterns found in Holocene river deposits (Pryor, 1973 and this study).

These include:

1) The tendency of precipitate bands to be influenced by the directional permeability gradients in cross stratified units (Figure 25 A and B),
2) The effect of discontinuous mudstone layers that disrupt flow patterns and result in an offsetting of precipitate bands (Figure 26 A and B),
3) The presence of fine bands of precipitate that parallel the cross laminations above the final precipitate (ore deposit) (Figures 27 A and B). Similar relations have been noted by Squyres (1963) in the Ann Lee Mine of the Grants mineral belt.
4) The large variability in textural and permeability patterns in Holocene point bar deosits which might result in the intonguing relations found in ore bearing sandstones of the Slick Rock district (Figures 25 A and B) and in some model experiments (Figure 24B).
5) The presence of remnant pods of ore bodies in altered tongues (Figure 24B).

Figure 25. (A) View of ore-bearing sandstones of the Salt Wash Member, Morrison Formation, underground mine, Slick Rock District, southwest Colorado. Note the tendency for the dark precipitate bands to be influenced or controlled by cross bed directions and permeability variations in different layers and the intertonguing relations of the light and dark colored rock.

(B) Sketch of ore-bearing sandstone of the Salt Wash Member, Morrison Formation, Slick Rock District, southwest Colorado. Note the intertonguing relation of the altered facies and the red-bed facies and the tendency for the interface between these two facies to be controlled by cross-laminations (detailed view) (from Shawe, 1976, p. D25).

A

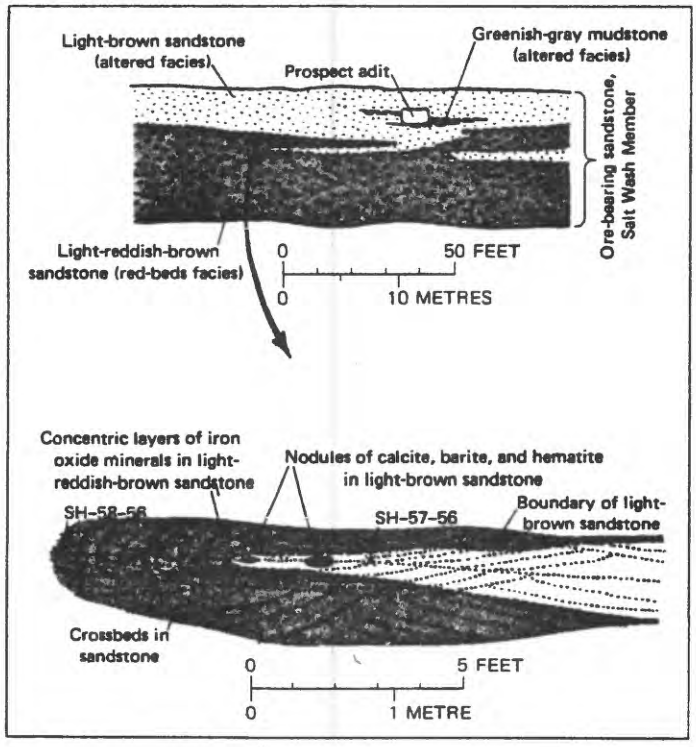
Light-brown sandstone (altered facies)
Prospect adit
Greenish-gray mudstone (altered facies)
Ore-bearing sandstone, Salt Wash Member
Light-reddish-brown sandstone (red-beds facies)
0
50 FEET
0
10 METRES
Concentric layers of iron oxide minerals in light-reddish-brown sandstone
Nodules of calcite, barite, and hematite in light-brown sandstone
SH-58-56
SH-57-56
Boundary of light-brown sandstone
Crossbeds in sandstone
0
5 FEET
0
1 METRE

B

A

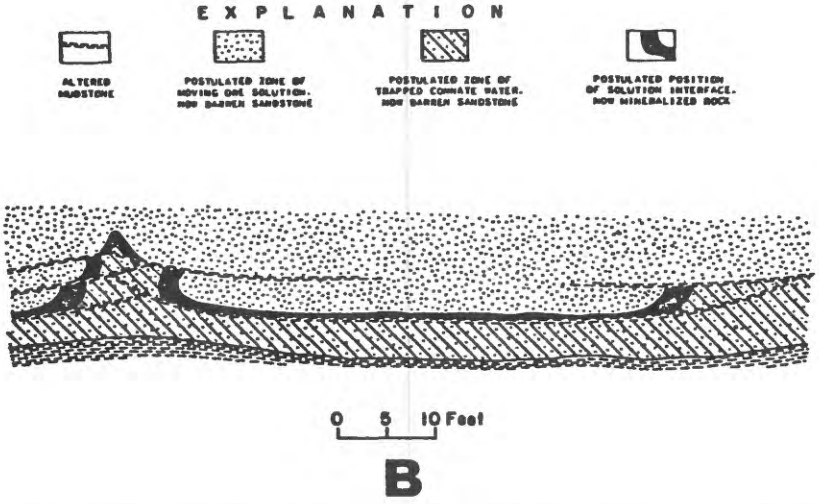

B

Figure 26 (A) Close view of a portion of the porous media flume (point X Figure 23A) showing the effects of mudstone layer on the precipitate band. Compare this view of the porous media to the cross section from Shawe, et al., (1959) in B below.

(B) Diagrammatic cross-section of rolls in sandstone layer near the base of the ore-bearing unit of the Salt Wash Member of the Morrison Formation, Cougar Mine, Slick Rock District, San Miguel County, Colorado (from Shawe, et al., 1959, p. 412).

Figure 27. (A) View of orebearing sandstone, Westwater Canyon Member, Morrison Formation, Ambrosia Lake Trend, Grants Mineral Belt, New Mexico. Note the sharp contact between the barren ground above and the dark ore zone below and the thin dark lines of precipitate that follow cross bed patterns in the light colored barren ground.

(B) Small-scale porous media flume showing the main precipitate band just above or at the lower horizontal layers (X) and the stringer of precipitate in the aluminum solution between the two horizontal layers (Y). These stringers of precipitate conform closely to the orientation of trough cross beds in this unit (Braided stream model, Run 27, Table 7). Flow direction indicated by large arrow.

A

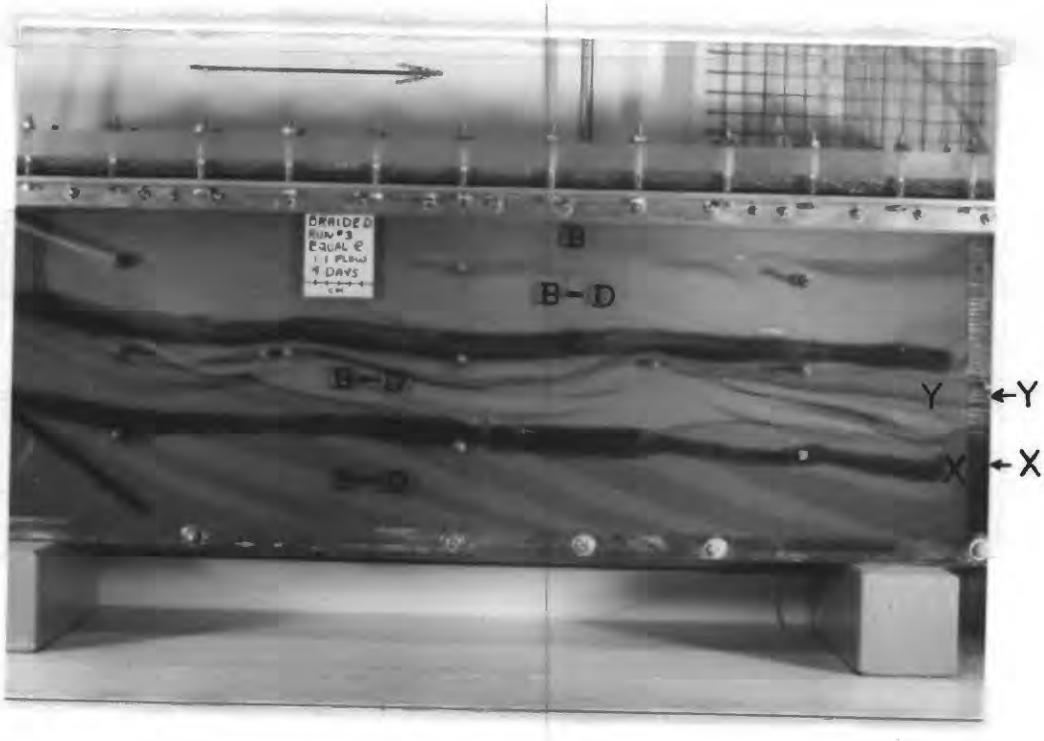

B

EFFECTS OF PRECIPITATE ON PERMEABILITY

In the first phase of this study it was demonstrated qualitatively that the precipitate has a tendency to fill the pores of the porous medium and reduce the hydraulic conductivity. In an attempt to quantify this effect a uniform flow of aluminum solution was initiated in a homogeneous porous medium consisting of Ottawa sand. A constant flow of humic acid was then injected at a point. Once the precipitate band was fully established, the flow of humic acid was stopped. Upon displacement of the humic acid by the aluminum solution a slug of dye was introduced simultaneously at three piezometer openings, located in a vertical plane, and their positions were recorded photographically at selected intervals of time. Figure 28 shows the position of the slugs of dye 20 minutes after they were introduced. It can be seen that the slug of dye enclosed in the precipitate band moves at a much slower rate. The difference in distance traveled by the slugs located inside and outside of the precipitate band is a measure of the relative reduction in conductivity caused by the clogging effect of the precipitate.

If we assume that the gradient that produced flow is approximately the same throughout the length of the model then by using the analysis for hydraulic conductivities in series, we can compute the approximate reduction in the hydraulic conductivity of the precipitate band by:

$$\frac{K_{medium}}{K_{ppt}} = \frac{L_t}{L_{ppt}} \left(\frac{V_o}{V_i} - 1 \right)$$

K_{ppt} is the hydraulic conductivity of the precipitate

K_{medium} is the hydraulic conductivity of the medium

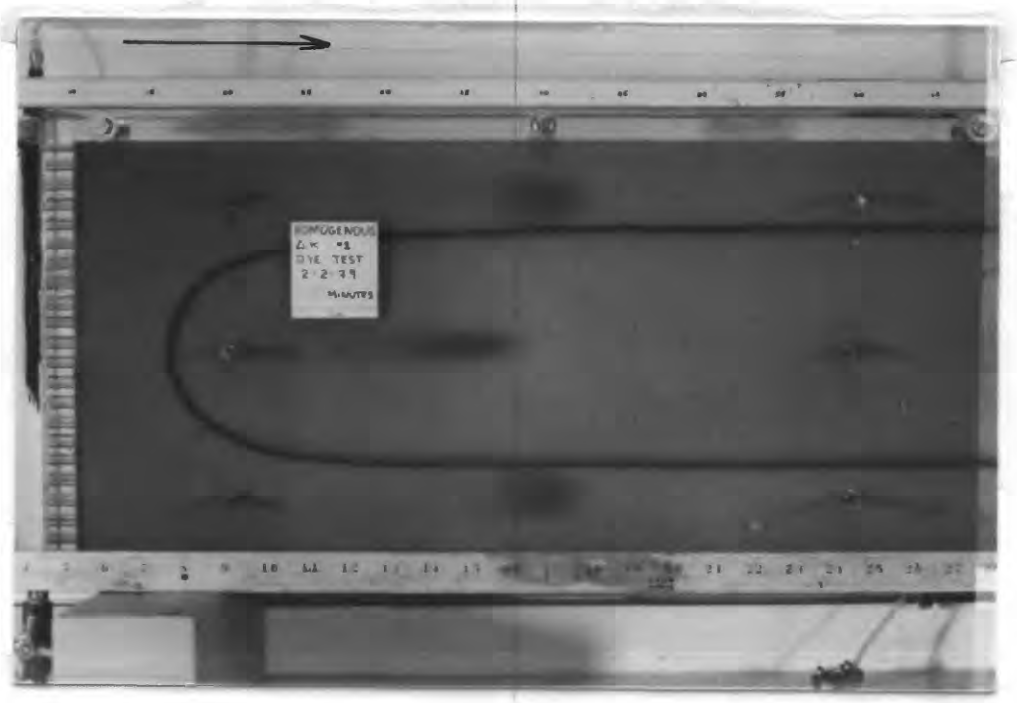

Figure 28. Small porous-media flume showing position of slugs of dye after 20 minutes. General flow direction indicated by large arrow.

L_t is the total length of the model

L_{ppt} is the thickness of the precipitate band

V_o is the velocity of the dye exterior to the precipitate band

V_i is the velocity of the dye enclosed by the precipitate

Using the data from the experiment shown in Figure 28 we obtain:

$$\frac{K_{medium}}{K_{ppt}} = \frac{35.5"}{(0.25)"} \left(\frac{1}{.75} - 1\right) = 47$$

This shows a tremendous reduction in hydraulic conductivity of the precipitate band. It should be noted that the reduction is local around the precipitate band.

NUMERICAL MODEL

A. Description of Numerical Model

A finite difference model called DEPOSIT was developed for the purpose of this study. The model employs a backward difference implicit scheme to predict transient, two dimensional potentiometric head fluctuations and the corresponding groundwater flows. Based upon these flows, the fully explicit mass balance technique was used to simulate the convective transport of the solution through the aquifer. Further details of the numerical model are presented by Ferentchak (1979).

B. Verification of Numerical Model

To verify the adequacy of the numerical model for predicting the shape and location of the interface, the results of the numerical model were compared to the results of the physical model. In addition, the numerical solution was compared to an analytical solution for the case of a line source in an aquifer.

Comparison with Analytical Solution and Physical Model - For the purpose of this comparison the penetration at a point of the aluminum solution into a uniform flow of the humic acid solution in a homogeneous porous medium composed of Ottawa sand, as presented in Table 7, Run 3, is considered.

The corresponding analytical solution may be obtained by superimposing the effects of a line source in a uniform flow field. The stream function describing the steady state flow pattern for the line source in an infinite uniform flow field may be written as (McWhorter and Sunada, 1977):

$$\psi = Kiy + \frac{Q}{2\pi b}\ \delta + \text{constant}\ ,\ \text{where:} \qquad (1)$$

ψ = stream function
i = uniform flow field gradient dh/dx
K = hydraulic conductivity of the medium
Q = discharge into the medium
b = thickness of the confined aquifer
δ = angle to point of desired stream function

$x \leq 0 \quad \delta = \pi - \arctan(y/x)$
$x > 0 \quad \delta = \arctan(y/x)$

Equation 1 was then used to obtain the location of the groundwater divide which is the position of the zero streamline and consequently the location of zero relative velocity between the two fluids. The zero streamline is of particular interest in our study since it was found in the porous media model that is corresponds to the location of the interface between the two solutions and hence, the position where the precipitate occurs. The basic solution to Equation 1 is appropriate for an aquifer of infinite areal extent. In order to compare the analytic solution with the results of the physical model, the method of images was used to account for the effects of imposed boundary conditions.

It should be noted that the analytic and numerical models simulate a fully penetrating line source and uniform flow which results in a two-dimensional flow field and, therefore, the flow pattern remains constant in the vertical direction (Figure 29). In the physical model the fluid was injected at a point source, thus affecting the flow field in the vertical direction and consequently resulting in a three-dimensional flow pattern. A cross-section of the pattern would approximate a semi-circle in a deep aquifer, but the actual situation in the physical model is truncated (Figure 29).

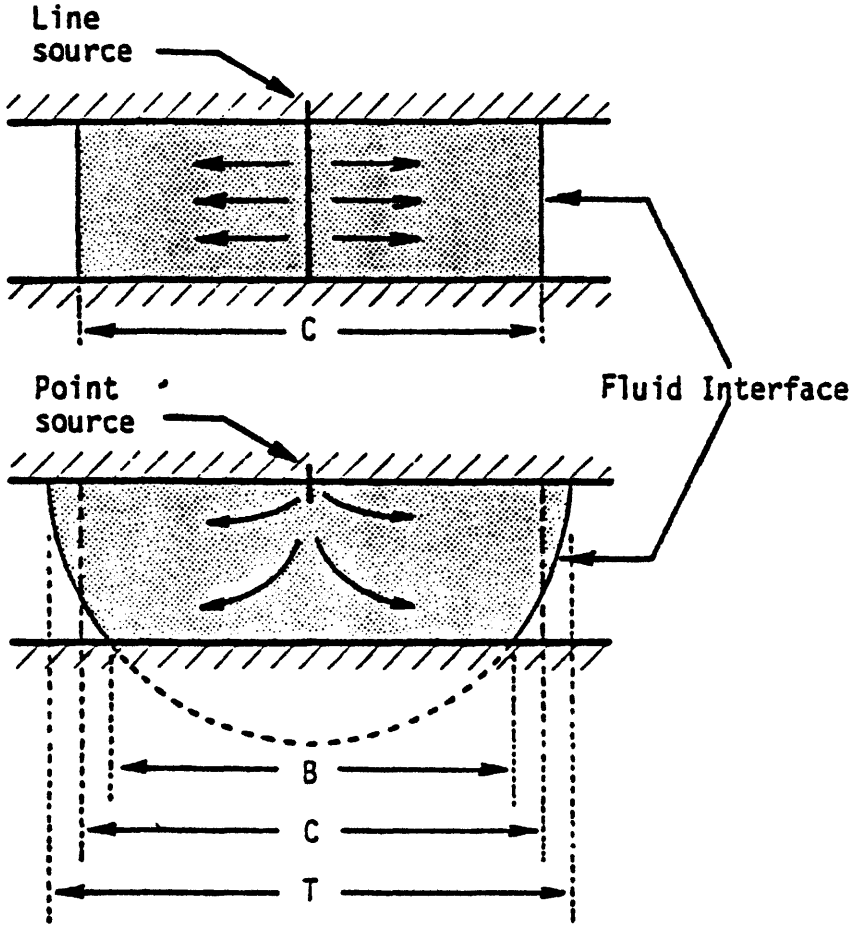

Figure 29. Fluid interfaces due to point and line sources (T, B, and C are the top, bottom, and constant cross-section dimensions respectively. C is the average of T and B).

For the purpose of the comparison an average of the top (T) and bottom (B) cross-sectional dimensions was used to approximate a constant cross-sectional dimension in the physical model for the case of injection of a line source instead of a point source. The resulting average profile (C, Figure 29) was then used to compare with the results obtained from the analytical and numerical models.

Figure 30 shows the comparison between the numerical and analytical solutions and the results obtained from Run 3 conducted in the physical model. The excellent agreement between the three solutions is indicative of the adequacy of the numerical model in predicting the shape and location of the interface and, hence, where precipitation occurs. It should be noted that the results from the numerical model were obtained from data on media properties determined in a separate laboratory test and not by calibrating the numerical model with the physical model. Further confirmation of the numerical model is presented by Ferentchak (1979). With additional research and calibration using data from non-homogeneous porous-media models and from actual uranium districts, the numerical model should prove helpful in predicting favorable sites for possible uranium mineralization.

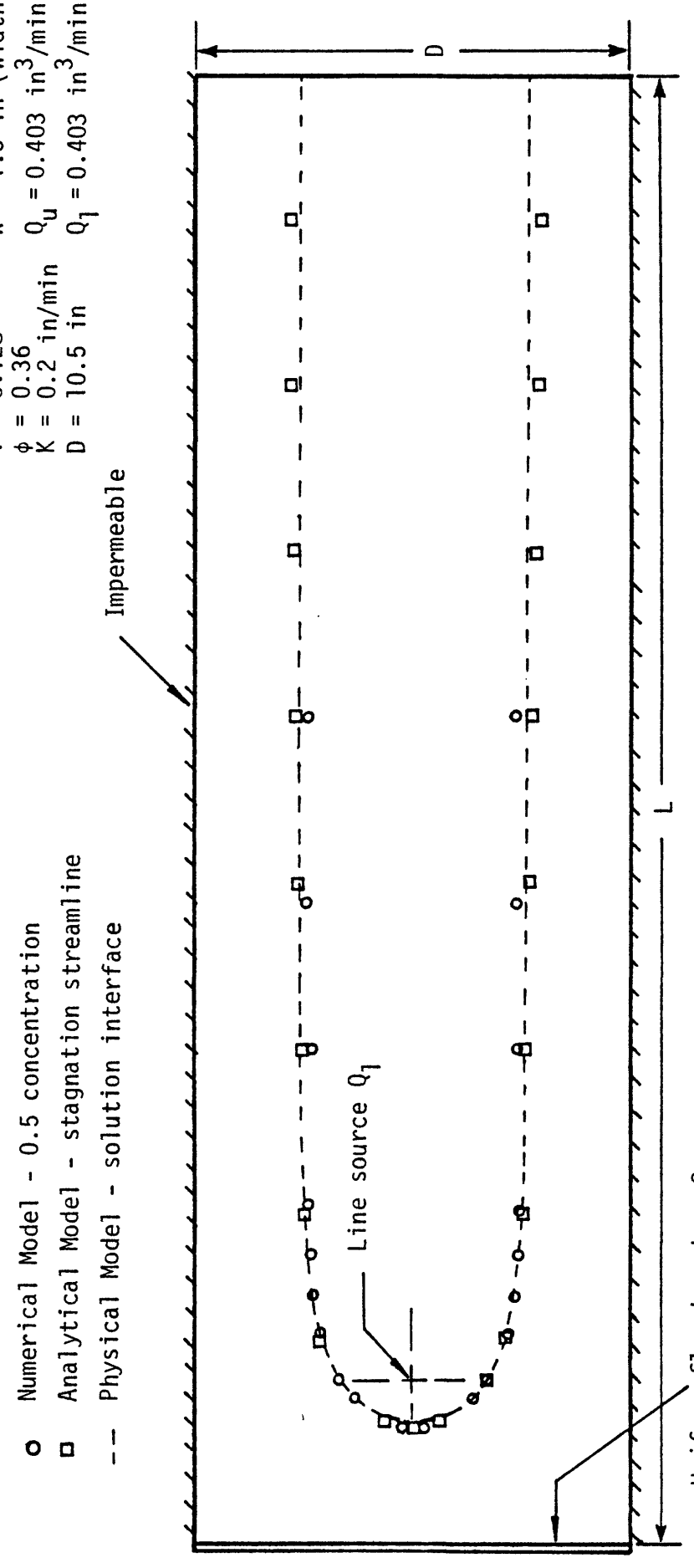

Figure 30. Comparison of three solutions for steady state conditions.

SUMMARY AND CONCLUSIONS

During the second phase of this study we have examined the textural, permeability, porosity and sedimentary structure patterns of Holocene point bar and braided stream deposits. Furthermore, it has been documented by our field studies and by an extensive review of the literature that the host sandstones of uranium ore in the Colorado Plateau have similar origins (e.g. braided and meandering stream deposits). The Westwater Canyon Member of the Morrison Formation in the Grants mineral belt was deposited as a coalescing system of braided channels possibly in a low gradient, wet alluvial fan while the Salt Wash Member of the Morrison Formation was deposited as point bars, channels and associated levees, crevasse splays, abandoned channels and floodplains in a river system.

Similarities between the model experiments of the two types of deposits and actual uranium deposits suggest that it is not unreasonable to call upon reactions at the interface between two solutions to produce the so-called tabular deposits of the Colorado Plateau.

If the ore forming processes were early in the post depositional history as suggested by many researchers, then the geometry and distribution of the ore deposits may have been largely controlled by the geometry and distribution of the channel deposits and the textural, porosity, permeability and sedimentary structure patterns within these units. In the second phase of this study we have examined only the detailed textural, permeability, porosity and structure patterns and their relation to the precipitate band (ore deposit). In the third phase we will attempt to examine the overall geometry and distribution of the host sandstone deposits and their relation to the ore deposits in physical model studies and in the Slick Rock

district in an extension of the work already undertaken by Shawe (1968).

As a final part of the second phase of this study an existing numerical model was modified and calibrated for use in predicting the shape and location of the interface between two solutions. Excellent agreement among the numerical, analytical and physical model solutions indicates the adequacy of the numerical model in predicting the shape and location of the precipitate band. In the third phase of the study the numerical model will be calibrated using field and model data and will be tested for its ability to predict favorable locations of uranium deposits.

REFERENCES

Allen, J. R. L., 1965a, Fining-upwards cycles in alluvial successions: Geol. Jour., v. 4, p. 229-246.

Allen, J. R. L., 1965b, A review of the origin and characteristics of Recent alluvial sediments: Sedimentology, v. 5, p. 89-191.

Bailey, R. V. and Childers, M. O., 1977, Applied mineral exploration with special reference to uranium: Westview Press, Boulder, Colorado 542 p.

Bernard , H. A., and Major, C. F., Jr., 1963, Recent meander belt deposits of the Brazos River: an alluvial 'sand' model: Bull. Am. Assoc. Petrol. Geol., v. 47, p. 350.

Beard, D. C. and Weyl, P. K., 1973, Influence of texture on porosity and permeability of unconsolidated sand: Am. Assoc. Petrol. Geol. Bull., v. 57, p. 349-369.

Campbell, C. V., 1976, Reservoir geometry of a fluvial sheet sandstone: Amer. Assoc. Petrol. Geol. Bull., v. 60, p. 1009-1020.

Craig, L. C.; Holmes, C. N.; Cadigan, R. A.; Freeman, V. L.; Mullens, T. E. and Weir, G. W., 1955, Stratigraphy of Morrison and related formations, Colorado Plateau region, a preliminary report: U. S. Geol. Survey Bull. 1009-E, p. 125-168.

Elliott, T., 1974, Interdistributary bay sequences and their genesis: Sedimentology, v. 21, p. 611-622.

Ethridge, F. G.; Ortiz, N. V.; Granger, H. C.; Farentchak, J. A. and Sunada, D. K., (in press), effects of groundwater flow on the origin of Colorado Plateau Type uranium deposits, in, Rautman, C. (ed.) New Mexico Bureau of Mines and Mineral Resources Memoir 38.

Falkowski, S. K., 1979, Geology and ore deposits of Johnny M mine, Ambrosia Lake District, N. M. (abs.): Symposium on Grants Uranium Region, Albuquerque, N. M., May 14-16, 1979.

Ferentchak, J. A., 1979, Investigation of the influence of ground water on sandstone type uranium deposits: unpub. M. S. thesis, Colorado State Univ., 110 p.

Fischer, R. P. and Hilpert, L. S., 1952, Geology of the Uravan mineral belt: U. S. Geol. Survey Bull. 988-A, p. 1-13.

Folk, R. L., 1974, Petrology of sedimentary rocks, Hemphill Pub. Co., Austin, Tx., 182 p.

Fraser, H. J., 1935, Experimental study of the porosity and permeability of clastic sediments: Jour. Geology, v. 43, p. 910-1010.

Galloway, W. E., 1978, Morrison Formation - Colorado Plateau, in, Galloway, W. E.; Kreitler, C. W.; and McGowen, J. H., Depositional and groundwater flow systems in the exploration for uranium: a research colloquium: Bur. Econ. Geol., The Univ. of Texas at Austin, p. X1-X15.

Galloway, W. E.; Kreitler, C. W.; and McGowen, J. H., 1978, Depositional and ground-water systems in the exploration for uranium: a research colloquium: Bur. Econ. Geol., The Univ. of Texas at Austin, (pages numbered by section).

Girdley, W. A.; Flook, J. E.; and Harris. R. E., 1975, Subsurface stratigraphy and uranium-vanadium favorability of the Morrison Formation, Sage Plain area, southeastern Utah and southwestern Colorado: U. S. Energy Research and Development Administration, Grand Junction, Colo., GJO-912-21, 97+ p.

Granger, H. C., 1968, Localization and control of uranium deposits in the southern San Juan Basin mineral belt, New Mexico-- an hypothesis: U. S. Geol. Survey Prof. Paper 600-B, p. 1360-1370.

Granger, H. C., 1976, Fluid flow and ionic diffusion and their roles in the genesis of sandstone-type uranium ore bodies: U. S. Geol. Survey Open-file Rept. 76-454, 26 p.

Granger, H. C., et al., 1961, Sandstone-type uranium deposits at Ambrosia Lake, New Mexico-- An interim report: Econ. Geology, v. 56,p. 1179-1209.

Granger, H. C. and Warren, C. G., 1979, The importance of dissolved free oxygen during formation of sandstone-type uranium deposits: U. S. Geol. Survey Open-file Rept. 79-1603, 22 p.

Graton, L. C. and Fraser, H. J., 1935, Systematic packing of spheres with particular relation to porosity and permeability: Jour. Geology, v. 43, p. 785-809.

Green, M. W. and Pierson, C. T., 1977, A summary of the stratigraphy and depositional environments of the Jurassic and related rocks in the San Juan Basin, Arizona, Colorado and New Mexico: New Mex. Geol. Soc. Guidebook, 28th Field Conf., San Juan Basin III, p. 147-152.

Huffman, C. A. and Lupe, R. D., 1977, Influences of structure on Jurassic depositional patterns and uranium occurrences, northwestern New Mexico: New Mexico Geol. Soc. Guidebook, 28th Field Conf., San Juan Basin III, p. 277-283.

Isachsen, Y. W.; Mitcham, T. W.; and Wood, H. B., 1955, Age and sedimentary environments of uranium host rocks, Colorado Plateau: Econ. Geol., v. 50, p. 127-134.

Krumbein, W. C. and Monk, G. D., 1942, Permeability as a function of the size parameters of sedimentary particles: AIME Tech. Pub. 1492.

McWhorter, D. B. and Sunada, D. K. 1977, Ground water hydrology and hydraulics: Water Resources Publications, Inc., Fort Collins, Co.

Miall, A. D. (ed.), 1978, Fluvial sedimentology: Canadian Soc. of Petrol. Geol., Memoir 5, 859 p.

Miall, A. D., 1978, Depositional models for braided alluvium, in, Miall, A. D. (ed.), Fluvial sedimentology: Canadian Soc. of Petrol. Geol., Memoir 5, 597-604.

Motica, J. E., 1968, Geology and uranium-vanadium deposits in the Uravan mineral belt, southwestern Colorado, in, Ridge, J. D. (ed.), Ore deposits in the U. S. 1933-1967: New York, Am. Inst. Mining, Metallurgical, and Petroleum Engineers, p. 805-813.

Mullens, T. E. and Freeman, V. L., 1957, Lithogacies of the Salt Wash Member of the Morrison Formation, Colorado Plateau: Geol. Soc. America Bull., v. 68, p. 505-526.

Ortiz, N. V.; Ethridge, F. G.; Ferentchak, J.; and Sunada, D. K., 1978, Laboratory experimental study of the origin of Colorado Plateau Type uranium deposits: Interim Report prepared for U. S. G. S Project No. 41-08-0001-G-429, for the period 10/1/77 to 12/15/78, Groundwater Section, Dept. Civil Eng., Colo. State Univ., Fort Collins, 36 p.

Picard, M. Dane and High, L. R., Jr., 1972, Criteria for recognizing lacustrine rocks, in, Rigby, J. K. and Hamblin, Wm. K., (eds.), Society of Econ. Paleo. and Mineral., Sp. Pub. No. 16, p. 108-145.

Pryor, W. A., 1973, Permeability-porosity patterns and variations in some Holocene sand bodies: Am. Assoc. Petrol. Geol. Bull., v. 57, p. 162-189.

Rackley, R. I., 1976, Origin of western-states type uranium mineralization, in, Wolf, K. H., (ed.), Handbook of strata-bound and stratiform ore deposits, vol. 7, Elsevier, N. Y., p. 89-156.

Reading, H. G. (ed.), 1978, Sedimentary environments and facies: Elsevier, New York, 557 p.

Saucier, A. E., 1976, Tectonic influence on uraniferous trends in the late Jurassic Morrison Formation, in, Woodward, L. A. and Northrop, S. A., (eds.), Tectonics and mineral resources of southwestern North America: New Mexico Geological Survey Sp. Pub. No. 6, p. 151-157.

Shawe, D. R., 1956, Significance of roll ore bodies in genesis of uranium vanadium deposits on the Colorado Plateau, in, Page. L. R., Stocking H. E. and Smith, H. B., Contributions to the Geology of Uranium and Thorium: U. S. Geol. Survey Prof. Paper 300, p. 239-241.

APPENDIX I

SOUTH PLATTE RIVER, LONGITUDINAL BAR #1
NEAR GOODRICH, COLORADO

SAMPLE NO.	PERM (darcys)	POROSITY %	MEAN GR. SIZE (mz) (ϕ)	MEDIUM GR. SIZE (ϕ)	SORTING	SKEWNESS	KURTOSIS	DIST. DOWNSTREAM (ft)
PROFILE SAMPLES								
L-1-27	86.52	40.00	-1.010	-1.347	1.712	0.310	0.713	0
L-1-26	68.53	42.10	-0.894	-1.252	1.956	0.236	0.654	1
L-1-25	36.01	37.60	-0.552	-0.407	1.985	-0.089	0.666	3
L-1-24	48.41	36.90	-0.755	-0.874	1.960	0.079	0.742	6
L-1-23	21.93	39.70	-0.345	-0.363	2.553	0.014	0.587	7
L-1-22	low	42.80	too open ended to calculate					7
L-1-18	9.18	39.70	1.323	1.606	1.565	-0.279	1.140	69
L-1-17	1.42	46.10	2.618	2.616	0.917	0.030	1.211	70
L-1-16	91.94	44.50	-0.360	-0.348	1.558	-0.005	0.814	71
L-1-15	48.64	37.60	-0.406	-0.429	1.796	-0.010	0.788	72
L-1-14	7.24	47.10	1.342	1.239	1.251	0.101	1.161	72
L-1-13	113.57	44.10	-0.699	-0.874	1.510	0.140	0.746	73
L-1-6	107.86	41.4	too open ended to calculate					146
L-1-5	67.95	38.8	-0.750	-0.991	2.020	0.102	0.708	148
L-1-4	108.54	41.9	-0.352	-0.441	1.466	0.103	0.895	149
L-1-3	97.43	44.2	0.297	0.203	1.107	0.101	0.956	151
L-1-2	4.27	41.6	-0.359	-0.366	1.544	-0.009	0.946	152
L-1-1	92.66	46.1	0.382	0.507	1.238	-0.168	0.822	154
L-1-12	94.58	43.4	1.792	1.685	0.920	0.134	1.411	191
L-1-11	90.73	42.6	-0.370	-0.369	1.768	-0.007	0.680	193
L-1-10	61.74	30.9	-1.205	-1.769	2.227	0.285	0.723	196
L-1-9	63.70	39.6	-0.510	-0.418	1.936	-0.064	0.645	199
L-1-8	100.73	44.2	-0.389	-0.471	1.817	0.013	0.724	204
L-1-7	189.52	46.7	-1.201	-1.428	1.656	0.173	1.147	206
GRID SAMPLES								
L-1-31	50.19	46.70	0.486	0.614	1.184	-0.146	0.799	156
L-1-38	77.92	47.30	too open ended to calculate					
L-1-39	2.00	45.50	2.570	2.625	1.097	-0.151	1.478	157
L-1-46	102.83	47.10	0.117	0.112	1.065	-0.044	0.949	158
L-1-32	101.36	49.40	0.170	0.207	1.307	-0.056	0.814	160
L-1-37	13.94	43.90	0.795	1.098	1.780	-0.250	0.853	161
L-1-40	9.87	42.00	1.150	1.244	1.388	-0.070	0.870	162
L-1-45	57.38	47.00	0.674	0.693	0.979	-0.029	0.862	162
L-1-33	78.77	44.70	-0.342	-0.369	1.339	0.008	0.828	165
L-1-36	91.80	46.00	-0.333	-0.370	1.540	-0.003	0.851	166
L-1-41	67.04	45.50	0.433	0.574	1.288	-0.183	0.819	167
L-1-44	26.35	45.00	1.069	1.533	1.286	-0.548	1.426	168
L-1-34	79.19	43.40	-0.416	-0.860	1.625	0.299	0.714	170
L-1-35	51.57	43.70	0.439	0.581	1.248	-0.190	0.989	171
L-1-42	35.70	46.10	1.310	1.225	0.783	0.148	1.559	172
L-1-43	26.33	45.40	1.429	1.607	1.014	-0.423	1.751	173
BEDDING UNIT SAMPLES								
L-1-19	8.13	53.6	2.579	2.577	0.596	0.031	1.475	73
L-1-20	10.32	42.2	1.593	1.598	1.465	0.007	0.996	73
L-1-21	44.32	42.4	0.243	0.501	1.496	-0.211	0.982	73
L-1-28	10.14	49.1	1.994	2.139	0.770	-0.248	1.096	73
L-1-29	low	52.7	2.762	2.664	1.146	0.111	1.287	73
L-1-30	27.32	43.5	0.748	1.018	1.370	-0.275	1.112	73

SOUTH PLATTE RIVER, LONGITUDINAL BAR #2
NEAR WELDONA, COLORADO

SAMPLE NO.	PERM (darcys)	POROSITY %	MEAN GR. SIZE (mz) (ϕ)	MEDIUM GR. SIZE (ϕ)	SORTING	SKEWNESS	KURTOSIS	DIST. DOWNSTREAM (ft)
PROFILE SAMPLES								
L-2-70	49.15	30.90	-1.484	-1.896	2.145	0 0.282	0.599	0
L-2-71	76.83	35.00	-1.214	-1.465	2.037	0.174	0.682	2
L-2-72	71.46	39.20	-0.443	-0.472	1.870	-0.016	0.666	3
L-2-73	6.77	31.60	-0.476	-0.787	1.835	0.237	0.781	4
L-2-74	14.96	27.10	too open ended for calculation					41
L-2-62	64.99	34.10	-0.832	-0.798	1.922	-0.029	0.703	31
L-2-63	52.62	38.20	-0.031	0.548	1.790	-0.401	0.636	32
L-2-64	20.55	37.00	-0.068	-0.326	1.814	0.180	0.701	34
L-2-65	50.95	38.60	-0.419	-0.447	1.551	-0.012	0.977	34
L-2-66	2.55	40.80	0.307	0.577	1.792	-0.151	0.848	35
L-2-51	16.92	41.00	1.046	1.667	1.450	-0.582	1.202	69
L-2-52	82.03	36.90	-1.248	-1.443	2.034	0.092	0.734	71
L-2-53	92.20	40.00	-0.845	-0.955	1.850	0.096	0.759	72
L-2-54	118.43	41.10	-0.874	-0.918	1.472	0.088	0.957	74
L-2-55	93.72	40.80	-0.530	-0.406	1.357	-0.107	0.944	75
L-2-47	23.80	42.60	0.136	0.177	1.795	-0.053	0.771	108
L-2-48	42.81	40.90	-0.661	-0.449	2.242	-0.077	0.616	108
L-2-49	5.63	48.10	1.104	2.066	2.217	-0.555	0.769	109
L-2-50	100.92	39.10	-0.851	-0.852	1.581	-0.038	1.097	109
GRID SAMPLES								
L-2-77	60.32	39.90	-0.220	-0.413	1.735	0.143	0.881	38
L-2-84	141.55	42.10	-0.771	-0.897	1.641	0.072	0.827	39
L-2 85	106.32	43.50	0.118	0.213	1.520	-0.170	0.985	40
L-2 92	95.97	40.20	-0.209	-0.306	1.652	0.020	0.851	40
L-2 78	57.36	39.90	0.250	0.650	1.749	-0.338	0.694	43
L-2 83	146.60	44.70	too open ended for calculation					
L-2 86	195.04	45.20	-0.913	-0.871	1.806	-0.056	0.784	44
L-2 91	97.11	44.00	0.109	0.168	1.455	-0.101	0.925	45
L-2 79	41.50	40.20	0.815	1.198	1.473	-0.411	1.263	48
L-2 82	85.30	45.10	-0.198	-0.286	1.620	0.034	0.809	49
L-2 87	202.23	45.50	-1.084	-1.327	1.483	0.220	0.991	49
L-2 90	122.11	42.70	-0.252	0.016	1.828	-0.223	0.878	50
L-2 80	68.05	40.80	0.419	0.563	1.273	-0.190	0.992	53
L-2 81	142.58	46.00	-0.380	-0.473	1.465	0.140	0.852	54
L-2 88	81.89	37.20	-0.586	-0.916	1.832	0.189	0.752	54
L-2 89	139.25	44.10	-0.300	-0.269	1.519	-0.049	1.004	55
BEDDING UNIT SAMPLES								
L-2-58	2.83	45.70	1.353	1.637	1.479	-0.245	0.998	2
L-2-59	102.97	41.20	-0.720	-0.851	1.623	0.072	0.832	2
L-2-75	33.75	35.90	-0.501	-0.393	2.056	-0.035	0.628	4
L-2-76	22.55	35.70	-0.181	-0.377	1.598	0.194	0.839	4
L-2-60	30.77	43.70	0.997	1.558	1.446	-0.519	0.958	4
L-2-61	71.52	40.50	-0.374	-0.751	1.662	0.245	0.688	4
L-2-93	74.44	40.10	0.009	0.623	1.778	-0.421	0.626	32
L-2-94	154.71	38.70	-1.277	-1.411	1.650	0.160	0.958	32
L-2-67	39.68	36.70	-0.685	-0.857	2.075	0.128	0.574	34
L-2-68	28.20	39.60	-0.047	0.048	2.090	-0.044	0.899	34
L-2-69	72.44	37.70	-0.404	-0.403	1.541	-0.008	0.935	34
L-2-56	37.53	42.10	1.368	1.524	0.858	-0.415	1.233	69
L-2-57	58.02	37.00	-0.072	0.049	1.294	-0.159	0.855	69